CHAPTER 2

EXPERIMENTAL TECHNIQUES AND ALLIED THEORY

2.1 INTRODUCTION

Liquid crystals have very interesting physical and optical properties which have been established by scientists around the world and various theoretical models have been developed over the years to explain their physical properties. A large variety of liquid crystalline materials have been synthesized and their properties have been determined to establish the relationship between the molecular structures and the macroscopic properties of the materials. A systematic study of the experimental techniques is required for measuring the physical, chemical, electro-optical and dielectric parameters of the compounds. In this dissertation, various properties of selected mesogenic compounds have been studied using different experimental techniques. A brief theoretical background of these techniques along with the Maier-Saupe mean-field theories of nematic and smectic A phases have been described, since most of the materials possess these two phases.

2.2 THEORIES OF LIQUID CRYSTALLINE PHASES

Liquid crystals are an important subclass of soft condensed matter self-assembled on nano scale level and can be broadly described as ordered fluids formed from geometrically anisotropic molecules. The main feature of a liquid crystal is that it is anisotropic in nature and this anisotropic behaviour complicates the analysis of these materials to a great extent. However there are a number of fairly simple theories that can at least predict the general behaviour of the liquid crystal systems. The first molecular field theory of the nematic phase was proposed by M. Born in 1916 [1] where he considered that the nematic medium is an assembly of permanent electric dipoles although it is now well established that the liquid crystalline molecules need not possess permanent dipole moment as a pre-requisite. Various molecular statistical theories have been developed over the years which have been dealt in the books - “The Physics of Liquid Crystals” by de Gennes [2], “Thermophysical Properties of Liquid Crystals” by Tsykalo [3], “Liquid Crystals” by Chandrasekhar [4], “The Physics of Ferroelectric and Antiferroelectric Liquid Crystals” by Musevic, Blinc and Zeks [5] and in books and monographs by various other authors.

Properties of the nematic phase of a liquid crystal can be studied extensively by the molecular field theory. The well known Maier-Saupe (MS) theory [6,7] which is based on the molecular field approximations, explains effectively the nematic isotropic (N-I) transition in

terms of the orientational order parameters. The first molecular statistical treatment of the smectic-nematic transitions was developed by Kobayashi [8], where he introduced an additional isotropic paired intermolecular interaction in Maier-Saupe (MS) model. A simple but elegant description of SmA phase was proposed by McMillan [9,10] in which he extended MS theory to include additional translational and mixed order parameters and characterized the layered structure of SmA phase. In the Kobayashi-McMillan approach the effects of short range order and fluctuation of the order parameters are neglected. The details of the McMillan, Wulf and de Gennes theories on SmC liquid crystals and the Meyer-McMillan theory on of SmC, SmB, and SmH liquid crystals are given in reference [11,12].

2.2.1 Order Parameter

Order parameter is a quantity that measures the amount of order present in a system. In case of rod like liquid crystals, the long molecular axis tends to align in a preferred direction called the director **n.** The orientational order parameter, in nematic phase, is basically used to describe the degree to which the liquid crystal molecules are oriented along that director. It can be described by averaged second order Legendre polynomial and is denoted by

$$S = \frac{1}{2}(3 < \cos^2 \theta > -1) \qquad (2.1)$$

where $< \cos^2 \theta >$ indicates a thermal average of all the molecules, θ being the angle between each molecule and the director. In crystalline state the molecules are perfectly oriented along the director and θ = 0 for each molecule, so S=1 for crystalline state. On the other hand in an isotropic liquid the molecules are randomly oriented and the thermal average results in S=0. Therefore, within liquid crystalline state S can vary between 0 and 1. The higher values of order parameters correspond to a more ordered phase, as temperature decreases the molecules becomes more ordered. In the absence of an external electric field the most common values of order parameters observed are from 0.3 and 0.9. Strictly speaking order parameter in nematic phase is described by a traceless symmetric tensor of rank two. In order to identify appropriate order parameters of the nematic liquid crystal, it is important to note that it is the probability distribution of the orientations of the constituent molecules that undergoes qualitative change due to change in the symmetry of the system.

Nematic liquid crystals possess uniaxial symmetry, i.e., in a homogeneous medium a rotation around the director does not make a difference. The observed symmetry and structure of the nematic liquid has established that a single order parameter will be sufficient to describe the structure of the phase. In case of smectic liquid crystals, formation of layered structures decreases the symmetry of the medium with respect to the homogeneities of the density, and hence such order parameter should be obtained from probability distribution of the molecular positions in addition to orientational ordering within a plane.

Maier-Saupe (M-S) Mean Field Theory of Nematic Phase

Maier-Saupe theory [6,13-16] is a molecular theory that may be considered with the behavior of one molecule in the field of other molecules. In nematic phase the individual molecule is affected by the anisotropic part of the dispersion interaction energy due to other neighboring molecules. Each molecule is assumed to be in an average orienting field due to its environment. A macroscopic sample contains a huge number of molecules and it is impossible to account for all possible interactions between them. W. Maier and A. Saupe [6] used the concept of orientational order in the nematic phase and approximated the electrostatic interaction by the first term of its multipole expansion. They considered that as far as long range nematic order is concerned, the influence of the permanent dipoles can be neglected and only the induced dipole-dipole interactions need to be considered. They also considered that for a given molecule the distribution of the centers of mass of the remaining molecules may be assumed to be spherically symmetric and the molecules are rotationally symmetric with respect to their long molecular axes.

Thus Maier-Saupe theory is based on the concept of an average potential which is employed to all molecules since every molecule is embedded in a sea of many other molecules, the idea utilized in a thermodynamic system called mean-field theory. The degree of alignment of the molecules with respect to the director **n** is described by an orientational order parameter given by (2.1).

It is noted that the potential energy corresponding to the alignment of the molecules is minimum when they are parallel to the director and maximum when they are perpendicular to the

director. The single molecule potential energy V_i should, therefore, be proportional to the function of $\cos^2\theta$ and the degree of order $< P_2 >$ and can be represented as

$$V_i(\cos\theta) \propto -\langle P_2(\cos\theta)\rangle P_2(\cos\theta)$$

$$V_i(\cos\theta) = -v\langle P_2(\cos\theta)\rangle P_2(\cos\theta) \qquad (2.2)$$

$$\text{i.e., } V_i(\cos\theta) = -\frac{A}{V_M^{\,2}}\langle P_2(\cos\theta)\rangle P_2(\cos\theta) \qquad (2.3)$$

where v is a factor represents the strength of intermolecular interaction, V_M is the molar volume of the sample and A is taken to be a constant independent of pressure, volume and temperature.

Humphries, James and Luckhurst [17] developed a more comprehensive concept by including higher order terms in the mean field potential for cylindrically symmetric molecules. Thus potential energy V was taken as

$$V_i(\cos\theta) = \sum_{L\,even} V_{Li}\langle P_L(\cos\theta)\rangle P_L(\cos\theta) \qquad (L\neq 0)$$

where $P_L(\cos\theta)$ is the L^{th} order Legendre polynomial.

Orientational Distribution Function and Evaluation of Order Parameters

Once the potential energy of a single molecule in the nematic phase is derived, the orientational distribution function [f(cosθ)] which gives the probability of finding a molecule at some prescribed angle θ from the director, can be obtained. According to classical statistical mechanics the orientational distribution function can be represented as

$$f(\cos\theta) = Z^{-1}\exp\left[\frac{-V(\cos\theta)}{kT}\right] \qquad (2.4)$$

where k is the Boltzmann constant, T is temperature in absolute scale and Z being the partition function for a single molecule. Z is given by

$$Z = \int_0^1 \exp\left[\frac{-V(\cos\theta)}{kT}\right] d(\cos\theta)$$

The order parameter <P_2> is the average value of the second order Legendre function for a given molecule and can be written as

$$S = \langle P_2 \rangle = \int_0^1 P_2(\cos\theta) f(\cos\theta) d(\cos\theta)$$

$$= \frac{\int_0^1 P_2(\cos\theta) \exp\left[v\langle P_2\rangle P_2(\cos\theta)/kT\right] d(\cos\theta)}{\int_0^1 \exp\left[v\langle P_2\rangle P_2(\cos\theta)/kT\right] d(\cos\theta)} \qquad (2.5)$$

This self-consistent equation can be solved numerically to find the temperature dependence of the order parameters. Out of several solutions, the equilibrium state is identified by the minimum value of free energy. For isotropic liquid <P_2>=0, which is the disordered phase. For T < 0.22284 v/k, equation 2.5 gives two other solutions. At absolute zero the upper branch tends to unity which represents nematic phase and the lower branch tends to $-\frac{1}{2}$ at absolute zero represents an unstable phase where the molecules attempt to orient themselves perpendicular to the director. From T = 0 to T = 0.22019 v/k the nematic phase is stable. Orientational order parameter varies from 1 at T=0 to 0.4289 at T=0.22019 v/k. Thus according to Maier-Saupe theory the nematic-isotropic transition is first order.

Exactly in a similar way one can find higher order orientational order parameter <P_4> using the 4th order Legendre polynomial in equation (2.5).

McMillan's Theory of Smectic A Phase

The theory of smectic A liquid crystals have been investigated by a number of investigators. McMillan's Theory [9] is an extension of the Maier-Saupe mean field model of nematics in which an additional order parameter characterizing the 1-D translational periodicity of the layered structure is included. Since the smectic A liquid crystals possess both orientational and translational order, the molecular distribution function must therefore describe both the

tendency of the molecules to orient along **n** and to form layers perpendicular to **n**. Thus the distribution function will be a function of both cosθ and z, and the normalised distribution function can be written as

$$f(z,\cos\theta) = \sum_{l\ even} \sum_{n} A_{l,n} P_l(\cos\theta)\cos(\frac{2\pi nz}{d}) \qquad (2.6)$$

with $$\int_{-1}^{1}\int_{0}^{d} f(z,\cos\theta)dz.d(\cos\theta) = 1 \qquad (2.7)$$

where d is the layer thickness.

The Kobayashi-McMillan (KM) description of the Sm_AN transition takes into account the effect of orientational order and an adhoc orientational interaction was introduced. In this theory the molecules are again assumed to be oriented along the z direction but the orientational ordering does not have to be ideal. With this concept McMillan developed [9] the theory of smectic A liquid crystals by assuming a model potential starting from the Kobayashi [18,19] form of potential. For simplicity, neglecting higher order terms, the mean field potential was expressed as

$$V_1(z,\cos\theta) = -v_0\left[\delta\alpha\tau\cos(\frac{2\pi z}{d}) + \left\{S + \sigma\alpha\cos(\frac{2\pi z}{d})\right\}P_2(\cos\theta)\right] \qquad (2.8)$$

where, $S = \frac{1}{2}\langle 3\cos^2\theta - 1\rangle$ is the orientational order parameter,

$\tau = \langle\cos(\frac{2\pi z}{d})\rangle$ is the translational order parameter, and

$\sigma = \langle P_2(\cos\beta)\cos(\frac{2\pi z}{d})\rangle$ is the mixed order parameter

and v_0 and δ are constants characterising the strengths of the anisotropic and isotropic parts of the interaction respectively, α is a parameter which depends on the core length and the molecular length. The above potential function reduces to MS potential when the two adjustable parameters δ and α become zero.

Here the distribution function can be expressed as

$$f_1(z,\cos\theta) = Z^{-1}\exp\left[-\frac{V_1(z,\cos\theta)}{kT}\right] \tag{2.9}$$

where the single molecular partition function Z is given by

$$Z = \int_0^d dz \int_0^1 \exp\left[-\frac{V_1(z,\cos\theta)}{kT}\right] d(\cos\theta)$$

The various order parameters are, shown to be, given by

$$\left.\begin{aligned} S &= \int_0^1\int_0^d P_2(\cos\theta)\, f_1(z,\cos\theta)dz.d(\cos\theta) \\ \tau &= \int_0^1\int_0^d \cos(\frac{2\pi z}{d})\, f_1(z,\cos\theta)dz.d(\cos\theta) \\ \sigma &= \int_0^1\int_0^d P_2(\cos\theta)\cos(\frac{2\pi z}{d})\, f_1(z,\cos\theta)dz.d(\cos\theta) \end{aligned}\right\} \tag{2.10}$$

These self-consistent equations can be solved numerically to find the temperature dependence of the three order parameters.

Out of several solutions, the equilibrium state is identified by the minimum value of free energy. In general we get the following three cases with S, σ and τ:

i) $\tau = \sigma = S = 0$, no order characteristic of the isotropic liquid phase;
ii) $\tau = 0$, $\sigma = 0$, $S \neq 0$, orientational order only, the theory reduces to the Maier-Saupe theory for the nematic phase; and
iii) $\tau \neq 0$, $\sigma \neq 0$, $S \neq 0$, orientational and translational order characteristic of the smectic A phase.

One can also predict the nature of the smectic to nematic phase transition observing McMillan ratio (T_{NA}/T_{NI}). If (T_{NA}/T_{NI}) > 0.87 then the SmA – N transition is of first order and if (T_{NA}/T_{NI}) < 0.87 then it is of the second order. Although the three quantities of equation 2.10 are sufficient

to parameterize simple mean field model, a good approximation to the true distribution function f(cosθ,z) requires many terms in equation 2.6.

2.2.2 Mesophase Structure: X-Ray Diffraction

X-ray diffraction study provides one of the most definitive ways to determine the structure of different liquid crystalline phases. Structural investigations of the mesophases, identification of different mesophases and study of various microscopic physical quantities can be studied by this method. An X-ray diffraction experiment gives Fourier image of the electron density function and analysis of those scattering data yields information about the mutual arrangement of the molecules in a particular liquid crystalline phase as well as the specific features of the orientational and translational long range order. The details of this technique have been reviewed by many authors [20-23].

Consider a basic scattering experimental technique as shown in Figure 2.1. Bragg visualized the scattering of X-rays by a crystal in terms of reflections from sets of lattice planes, as shown in Figure 2.2.

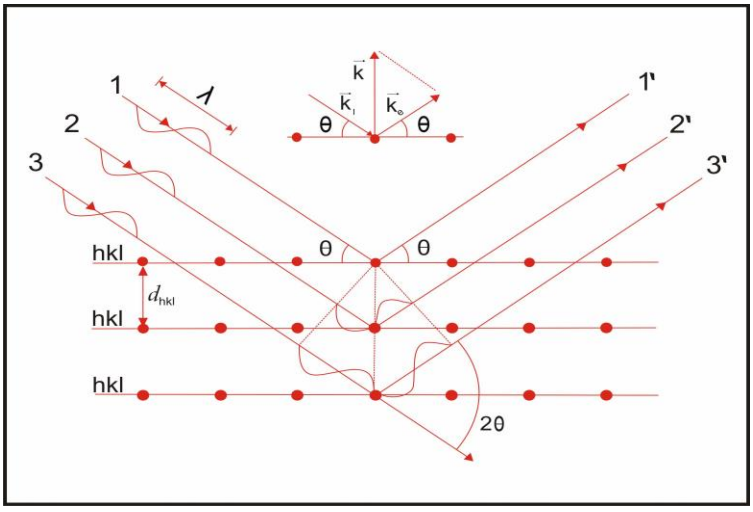

Figure 2.1: Typical scattering geometry showing the incident and scattered wave vector

For elastic scattering, the magnitude of incident and scattered wave vectors must be equal, i.e., $|\mathbf{K}_s| = |\mathbf{K}_i| = 2\pi / \lambda$, where λ is the wavelength of the incident radiation. The magnitude of the scattering wave vector is given by,

$$\mathbf{Q} = \mathbf{K}_s - \mathbf{K}_{i,.} \qquad Q = \left|\mathbf{Q}\right| = 4\pi\sin\theta/\lambda,$$

where 2θ is the angle between $\mathbf{K}_s$ and $\mathbf{K}_i$. The scattering of incident radiation by a scattering centre at $\mathbf{r}$ is described (relative to the initial amplitude) by the scattering amplitude $f \exp(i\mathbf{Q}.\mathbf{r})$, where f is the scattering power of the scattering centre. Generalised to N such scattering centres the scattering amplitude can be expressed as

$$F(\mathbf{Q}) = \sum_{j=1}^{N} f_j \exp(i\,\mathbf{Q}.\mathbf{r}_j) \qquad (2.11)$$

where $\mathbf{r}_j$ denotes the position of the j^{th} scattering centre. For a continuous distribution of scattering centers characterized by the electron density function $\rho(\mathbf{r})$ one writes

$$F(\mathbf{Q}) = \int \rho(\mathbf{r}) \exp(i\mathbf{Q}.\mathbf{r}) d\mathbf{r} \qquad (2.12)$$

If the integration is carried over all space then $\mathbf{F}$ is Fourier transform of the electron density and provides the link between the real ($\mathbf{r}$) and the reciprocal ($\mathbf{Q}$) space.

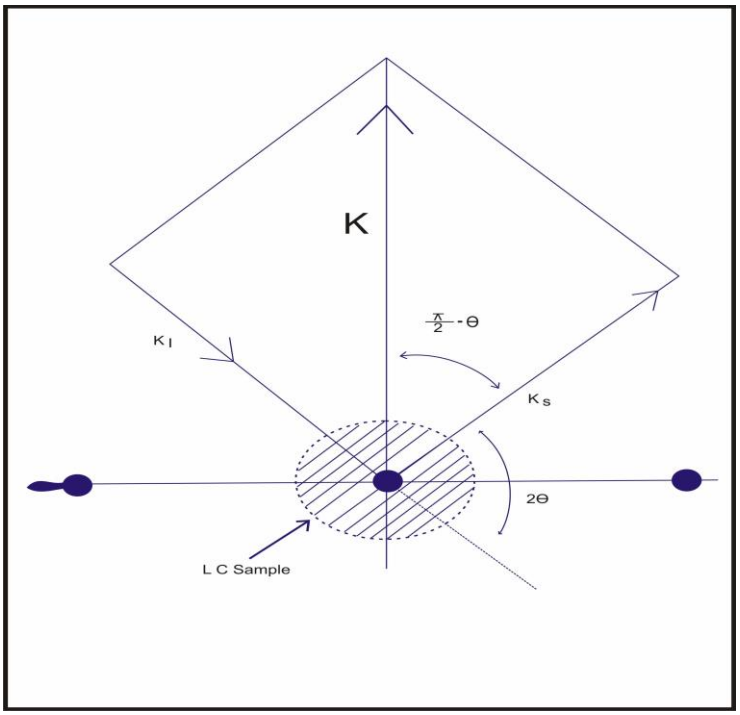

Figure 2.2: Typical scattering geometry showing the incident (K_i) and scattered (K_S) wave vector

For the case of isolated atom this assumes the form

$$f(\mathbf{Q}) = \int \rho_a(\mathbf{r}) \exp(i\mathbf{Q}.\mathbf{r}) d\mathbf{r}$$

which is called the atomic scattering amplitude. For a group of atoms, for which

$$\rho(\mathbf{r}) = \sum_{j=1}^{N} \rho_j(\mathbf{r} - \mathbf{r}_j)$$

this leads to

$$F(\mathbf{Q}) = \sum_{j=1}^{N} f_j(\mathbf{Q}) \exp(i\mathbf{Q}.\mathbf{r}_j) \qquad (2.13)$$

This is almost identical to equation (2.11), but in this case the atoms are considered as extended object and the variation of the atomic scattering amplitude with **Q** has been considered, i.e., the

diffraction by a set of atoms may be treated in terms of diffraction by a set of points, provided the variation of the atomic scattering amplitude is accounted for.

So far only scattering amplitudes have been considered. To get absolute value and hence the experimentally relevant intensity, the amplitude of a wave scattered by a single point electron must be known. With the help of classical electrodynamics expressing all intensities in terms of the scattering intensity of an electron we get expression for intensity

$$I(\mathbf{Q}) = \left| F(\mathbf{Q}) \right|^2$$

For molecular liquids it is convenient to separate the amplitude due to the molecular structure from the total scattering amplitude [13]. Accordingly equation 2.11 can be written as

$$F(\mathbf{Q}) = \sum_{k,m} f_{km}(\mathbf{Q}) \exp[i\,\mathbf{Q}.(\mathbf{r}_k - \mathbf{R}_{km})] \qquad (2.14)$$

where $\mathbf{r}_k$ gives the position of the centre of mass of the molecule 'k', and $\mathbf{R}_{km}$ is the position of the atom 'm' within that molecule, f_{km} is the atomic scattering factor of the atom 'm' in the molecule 'k'. Using (2.14) the general scattering intensity from a set of molecules is

$$I(\mathbf{Q}) = \sum_{k,l,n,m} \left\langle\ f_{k,m}(\mathbf{Q}) f^{*}_{ln}(\mathbf{Q}) \exp\left[i\,\mathbf{Q}.(\mathbf{r}_k - \mathbf{r}_j)\right] \exp\left[i\,\mathbf{Q}.(\mathbf{R}_{ln} - \mathbf{R}_{km})\right] \right\rangle \qquad (2.15)$$

where the brackets indicate statistical average over the constituent molecules of the liquid. The intensity given in equation 2.15 can be written as

$$I(\mathbf{Q}) = I_m(\mathbf{Q}) + D(\mathbf{Q})$$

where $I_m(\mathbf{Q})$ is the molecular structure factor and $D(\mathbf{Q})$ is called the interference function which are respectively given by

$$I_m(\mathbf{Q}) = \sum_k \left\langle \sum_{m,n} f_{km}(\mathbf{Q}) f^{*}_{kn}(\mathbf{Q}) \exp\left[i\mathbf{Q}.(\mathbf{R}_{kn} - \mathbf{R}_{km})\right] \right\rangle$$

$$= \mathbf{N}\langle \left| \sum_{m} f_{km} \exp(-i\,\mathbf{Q}.\mathbf{R}_{km}) \right|^2 \rangle \qquad (2.16)$$

$$D(\mathbf{Q}) = \langle \sum_{k \neq l} \exp(i\,\mathbf{Q}.\mathbf{r}_{kl}) \sum_{m,n} \langle f_{km}(\mathbf{Q}) f^{*}_{ln}(\mathbf{Q}) \exp[\mathbf{Q}.(\mathbf{R}_{ln} - \mathbf{R}_{km})] \rangle \rangle \qquad (2.17)$$

where $\mathbf{r}_{kl} = \mathbf{r}_k - \mathbf{r}_l$

The term $I_m(\mathbf{Q})$ gives the scattered intensity which would be observed from a random distribution of identical molecules. D(Q) is the term containing information about correlation in both positional and orientation of different molecules. The parameters are (i) apparent molecular lengths in nematics, (ii) layer thickness in smectics, (iii) average lateral distance between the molecules, (iv) correlation lengths, (v) tilt angle, (vi) molecular packing, (vii) orientational distribution function, (viii) order parameters $\langle P_2 \rangle$, $\langle P_4 \rangle$ ... etc., (ix) bond orientational order parameter, (x) layer order parameters τ and $\langle z^2 \rangle$ in Sm-A and (xi) critical exponents.

2.2.3 Identification of Mesophases and Transition Temperatures

The existence of a liquid crystalline phase can be established by visual inspection of the compound while it is heated. The mesophase is distinguished from the isotropic liquid by its turbid appearance and from the crystalline solid by its flow properties. A liquid crystal may possess a variety of mesophases which is impossible to identify only by visual inspection. To study a liquid crystal it is very important to identify its phase behavior and the transition temperatures of each phase. In order to identify the liquid crystal phases and to determine the corresponding transition temperatures, several techniques can be used. We have used three techniques viz. (1) Optical polarization microscopy (OPM), (2) Differential scanning calorimetry (DSC), (3) X-ray diffraction method, which is described in subsequent sections. Other techniques used to find the nature of a mesophase include neutron scattering [24], nuclear magnetic resonance (NMR) [24-26], IR, Raman, UV-Visible spectroscopic studies [27], Fabry-Perot Etalon method [28] etc.

Optical Polarization Microscopy (OPM)

The polarizing microscope (Figure 2.3) is a classical and very useful tool for the investigation of liquid crystalline phases. In an optical microscope one looks at the object image of a thin mesomorphic layer (thickness ~ 10-20 μm) between two glass plates under polarised light. The patterns so observed through the microscope are called textures which are due almost entirely to the defect structure that occurs in the long-range molecular order of the liquid crystals. Depending on the boundary conditions and the type of phase, specific textures are observed, that provide a means of classifying the different phases. The temperature of the liquid crystalline material is controlled usually between room temperature and 300^{o}C by inserting the glass slide in a hot stage and placed between the polarisers which are crossed at 90^{o} to each other. In isotropic phase the field of view appears dark, but beautiful texture appears if the material form liquid crystal phase on cooling. Observed texture type depends on the alignment of the sample viz., whether homeotropic or homogeneous (planar) and the involved phase structure.

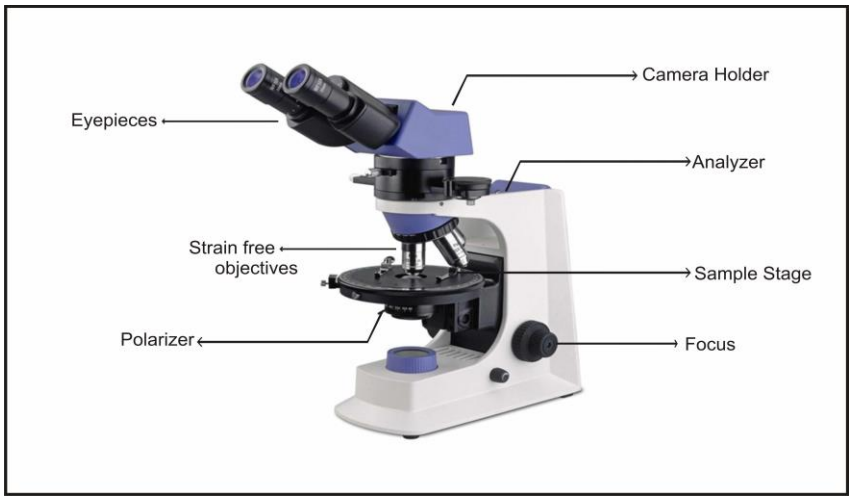

Figure 2.3: Polarizing microscope

Usually texture changes occur at the transitions between the various phases. A number useful books with photographs of typical textures and explanations of their origins have been published by Demus and Richter (1978) [29], I. Dierking [30], Slaney *et al.*[31] and Bouligand [32]. The identification of the mesophases by this technique is often difficult because similar textures might be exhibited by different phases or sometimes very subtle change in textures occur

at transitions and hence requires the support of other techniques to finalize the phase type present.

Differential Scanning Calorimetry (DSC)

Differential scanning calorimetry is the modern calorimetric method which is now very well-established tool for studying mesomorphic systems. The process reveals the transition temperatures of different phases by measuring the enthalpy change associated with a transition. The level of enthalpy change provides some indication of the types of phase involved. When a material melts, a change of state occurs from solid to liquid and this melting process requires energy (endothermic) from the surroundings. Converse is also true. Crystalline solid to liquid crystalline phase transition involves high enthalpy change (~30-40 $kJmol^{-1}$). But transition between two mesophases and mesophase to isotropic liquid transition are accompanied by much smaller enthalpy changes (~1-2 $kJmol^{-1}$). Mettler FP82 hot stage and FP84 thermosystem were used for texture and DSC studies. The DSC measurement setup is shown in Figure 2.4. A drawback of scanning calorimetric method is that the latent heat and the pretransitional increase in the specific heat near a phase transition are lumped together into one peak. In order to establish the nature of a phase transition the true latent heat must be measured. This can be done by adiabatic calorimetry, which is much more time consuming.

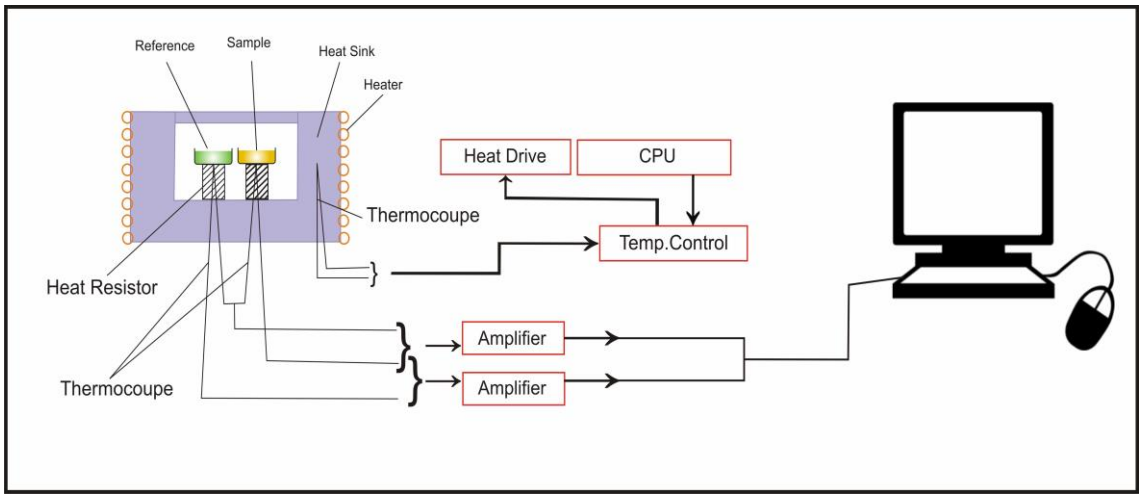

Figure 2.4: Experimental setup for DSC measurement

Experimental Techniques for X-ray Diffraction Studies and Method of Data Analysis

The basic experimental arrangement used for X-ray diffraction studies is shown in Figure 2.5 and similar experimental setup was designed and fabricated in our laboratory earlier [33,34], which I have used for the measurements.

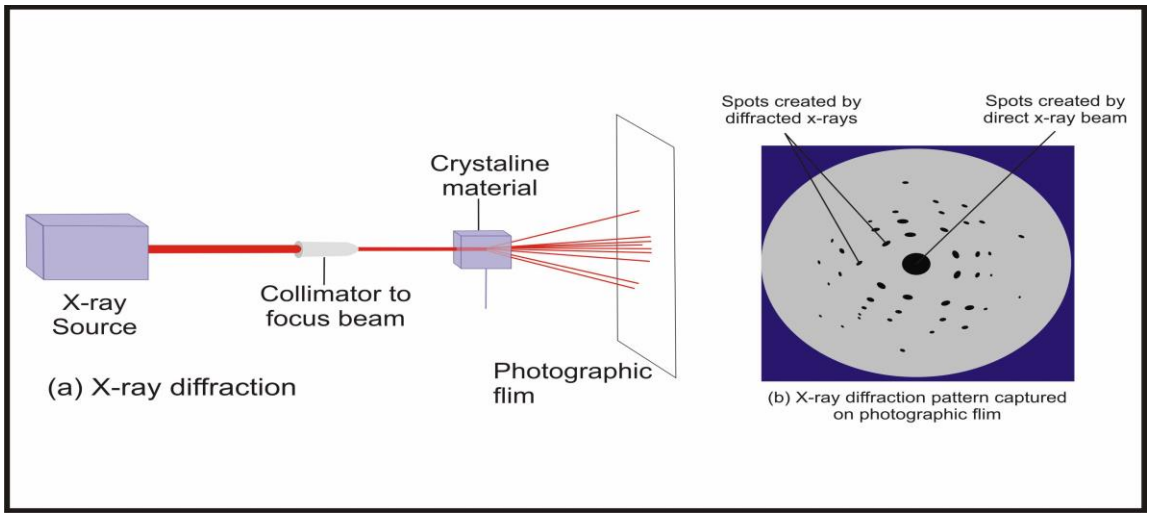

Figure 2.5: X-ray diffraction experimental setup and diffraction photographs

The x-ray diffraction photographs are taken using nickel filtered CuK_{α} radiation, in a flat plate camera. By capillary action the sample is filled in a thin walled (~0.05 mm) Lindemann glass capillary of 1 mm diameter and is aligned by slow cooling from the isotropic phase to the desired temperature. X-ray photographs were taken at different temperatures by using a temperature controller, Indotherm 401- (India) within an accuracy of $\pm 0.5^{0}$C and by the Eurotherm controller (2216e) with an accuracy ±0.1°C.

Various types of diffraction patterns are obtained depending upon the type of the mesophases [34-43]. For the discussion of the experimental results for X-ray scattering by nematic and smectic liquid crystals, typical diffraction photographs of magnetically oriented samples are shown in Figure 2.6.

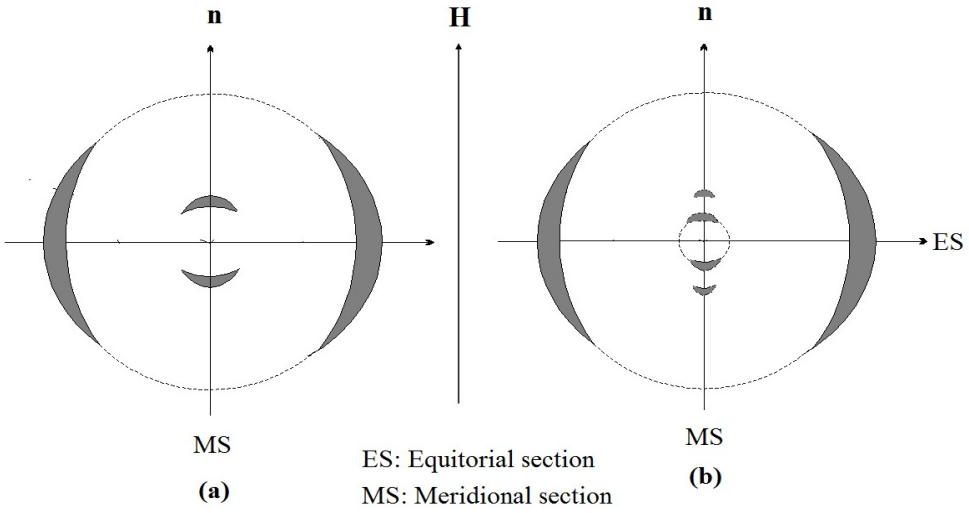

Figure 2.6: Schematic representation of the X-ray diffraction pattern of an oriented (**a**) nematic and (**b**) smectic A phase.

The diffraction pattern of nematic phase consists of a combination of meridional and equatorial maxima. However, an un-oriented nematic sample shows diffraction pattern as obtained from an isotropic liquid viz. two uniform halo, at low and high angles. This is due to the fact that, generally an un-oriented liquid crystal sample consists of a large number of domains and within each domain the molecules are aligned in a preferred direction, but there is no preferred direction for the sample as a whole and naturally, X-ray diffraction pattern will have a symmetry of revolution around the direction of X-ray beam. For an aligned nematic sample the outer circular halo is splitted into two crescents having maxima along the equatorial direction ($\perp$ to n) which are formed due to intermolecular scattering and the corresponding Bragg's angle is a measure of the lateral intermolecular distance (D). Generally the intermolecular distance (D) lie between 3.5Å to 6.5Å, lateral dimensions of a typical mesogenic molecule and the average intermolecular distance is found to be around 5Å. Along the meridional direction ($\parallel$ to **n**), the inner halo also has two crescents with maxima at much lower angle. This diffraction peak must arise from correlations in the molecular arrangement along the director **n**. So by measuring the corresponding diffraction angles one gets the value of the apparent molecular length (*l*) in the nematic phase and layer spacing in smectic phase. In case of smectic phases the inner pattern appears as sharp spots; sometimes second order spots are also found, translational order parameter can also be determined in such cases.

The average lateral distance between the neighboring molecules (D) was calculated from the x-ray diffraction photographs by using the Bragg formula

$$2D \sin\theta = k\lambda \qquad (2.18)$$

where θ is the Bragg angle for the equatorial diffraction, λ is the wavelength of the x-ray beam and 'k' is a constant which comes from the cylindrical symmetry of the system. For perfectly ordered state k =1.117 as given by de Vries [44,45]. As the variation of 'k' with $<P_2>$ is very small, the value of k = 1.117 is used for all our calculations. The apparent molecular length or the layer thickness 'd' is calculated from the equation

$$2d \sin\theta = \lambda \qquad (2.19)$$

where θ is the Bragg angle for the meridional diffraction crescents for an aligned sample and inner halo for unaligned sample.

For the determination of the actual distance between the sample and the film, x-ray diffraction photograph of aluminium powder was taken. The Bragg's angle θ′ corresponding to the (hkl) reflecting plane, is determined by using [46]

$$\sin\theta' = \frac{\lambda}{2a}\sqrt{h^2 + k^2 + l^2} \qquad (2.20)$$

where a is the lattice constant. Measuring the diameter of the diffraction rings corresponding to (111) and (222) reflections, the actual distance between the sample and the film was found out from the relation

$$\tan 2\theta' = \frac{R}{2H} = \frac{\text{radius of the ring}}{\text{sample to film distance}} \qquad (2.21)$$

Using this sample to film distance the Bragg angle (θ) for the peak corresponding to the parameters *l,d* and D of the liquid crystal sample were calculated using the above relation (2.21).

For the above analysis the diffraction photographs were first digitized in 24 bit RGB colour format by using HP scan jet 2200c scanner. The digitized images were analyzed using the colour values of the pixels to obtain the radii of the inner and outer diffraction rings and from that the apparent molecular length (*l*) or the smectic layer spacing (d) and the average intermolecular spacing (D) were obtained. Two softwares Adobe Photoshop 7.0 and origin 7.0 were used for analyzing the digital images. The uncertainties in calculated *l* and D values are ± 0.1, ± 0.02 Å respectively.

Synchrotron X-ray Diffraction

In Synchrotron X-Ray Powder Diffraction technique, X-rays are generated by a synchrotron facility and it is an extremely powerful source of X-rays. A synchrotron uses powerful magnets and radio frequency waves to accelerate charged particles. The powerful magnet and radio frequency waves accelerate negatively charged electron along a stainless steel tube, where they reach high speed. As the magnets are turned on and off, electrons get pulled along the ring of tubes. Since the fast-moving electrons emit a continuous spectrum of light, with various wavelengths and strength, scientists can pick whatever wavelength they need for their experiments e.g. visible light, ultraviolet light or X-rays (soft or hard x-rays). The X-rays thus produced are at least 5 orders of magnitude more intense than the best X-ray laboratory sources. For studying the structures of different phases in the chiral compound (MPOBC), synchrotron radiation facility, PETRA III beamline at P07 Physics Hutch station at DESY, Hamburg was used (Figure 2.7). A sample was taken in a Lindemann glass capillary of diameter 1.0 mm and very slowly cooled down from isotropic phase to the desired temperature to get an aligned sample. 50 images of exposure time 0.2 s were grabbed and averaged to get one diffraction image and five such images were collected at a particular temperature. All the physical parameters were averaged over these five image data. A Perkin Elmer 2D detector of pixel size 200 × 200 μm and total size 400 × 400 mm was used for image grabbing which was placed 3.3m away from the sample. QXRD program for PE Area Detectors (G Jennings, version 0.9.8, 64 bit) was used for data acquisition and also for analyzing the images. Images were integrated using a step size of 0.002 to get intensity versus wave vector (Q) distribution.

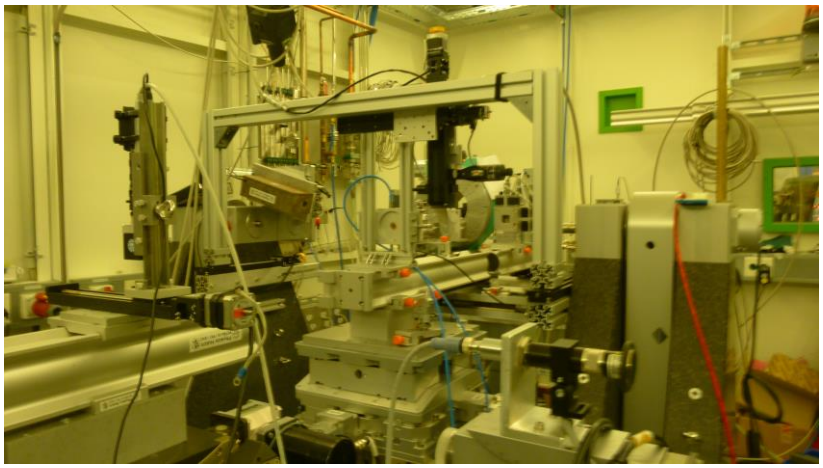

Figure 2.7: Synchrotron X-ray diffraction set up at DESY, Hamburg, Germany

2.2.4 Optical Birefringence

Liquid crystals are found to be birefringent due to their anisotropic nature i.e., they demonstrate double refraction. This is because of light polarized parallel to the director has a different index of refraction than light polarized perpendicular to the director. So, a uniaxial (liquid) crystal has two principal refractive indices, n_o and n_e. n_o is called the "ordinary" refractive index, associated with a light wave where the electric vector vibrates perpendicular to the optical axis. The "extraordinary" index n_e is observed for a linearly polarized light wave where the electric vector is parallel to the optical axis. The optical anisotropy or birefringence of a material is characterized by the difference ($\Delta n = n_e - n_o$) in the indices of refraction for the ordinary and extraordinary rays, which depends on the wavelength of the light used and the thermal state of the compounds [47]. Birefringence is a property usually associated with transparent crystals with a non-centrosymmetrical lattice structure. Physical origin of the optical properties of liquid crystal has been detailed by Dunmur [48].

Optical birefringence (Δn) is responsible for the appearance of interference colors in LCDs operating with plane-polarized light [49]. Interference between the extraordinary ray and the ordinary ray, gives rise to the colored appearance of these thin films. For a wave at normal incidence, the phase difference in radians between the o-ray and e-rays caused by traversing a

birefringent film of thickness d and birefringence Δn is referred to as the optical retardation δ given by

$$\delta = \frac{2\pi\Delta nd}{\lambda}$$

where λ is the wavelength of light in vacuum.

Measurement of Ordinary and Extraordinary Refractive Indices

The ordinary and extraordinary refractive indices (n_o, n_e) have been measured by constructing a thin prism in our laboratory. Geometry of the experimental set up is shown in Figure 2.8. To construct the prism a set of glass plates were taken and washed by concentrated nitric acid and clean water. After drying, plates were washed with acetone to clean oily substances present. The plates were then treated with a dilute (~1% aquas) solution of polyvinyl alcohol (PVA) and then dried and rubbed several times on a tissue paper in the same direction to get a preferential direction on the substrates. A prism was then formed, by keeping the treated surfaces inside and the rubbing directions parallel to the refracting edge of the prism. The sides of the prism were then sealed by using a high temperature adhesive and it was baked for several hours. The angles of the prisms were kept less than 1° by using a thin glass spacer. The details of the preparation of the prism are already reported by Zeminder *et al*. [50]. The prism was filled with sample in isotropic phase from its top open side such that no air bubble was trapped inside. The system was heated to isotropic phase and cooled down slowly to the desired temperature so that liquid crystalline molecules were perfectly aligned with its optical axis parallel to the refracting edge of the prism. The prism was then placed inside a laboratory made thermostatic brass oven with a circular aperture. The temperature of the oven was controlled by a temperature controller (Eurotherm model 2216e with an accuracy of ±0.1^{o}C). The refractive indices were measured by using a Laser source (Jain Lasertech Pvt. Ltd., India), a collimator and a transparent scale as screen placed at a large distance. By measuring the deviation produced by the ordinary ray and extraordinary ray, the corresponding refractive indices were measured. The ordinary refractive index (n_o) is temperature dependent, increasing slightly over the nematic range and then rapidly increases as the temperature nears the phase transition. Conversely, the extraordinary refractive index (n_e) is particularly dependent on the molecular structure and can

vary in the visible region from 1.5 for saturated compounds up to 2.0 for highly conjugated compounds. At temperatures above the clearing point (Tc), liquid crystals become isotropic liquids and birefringence goes to zero as n_e and n_o coincide at their mean. Measured refractive indices were accurate within ± 0.001.

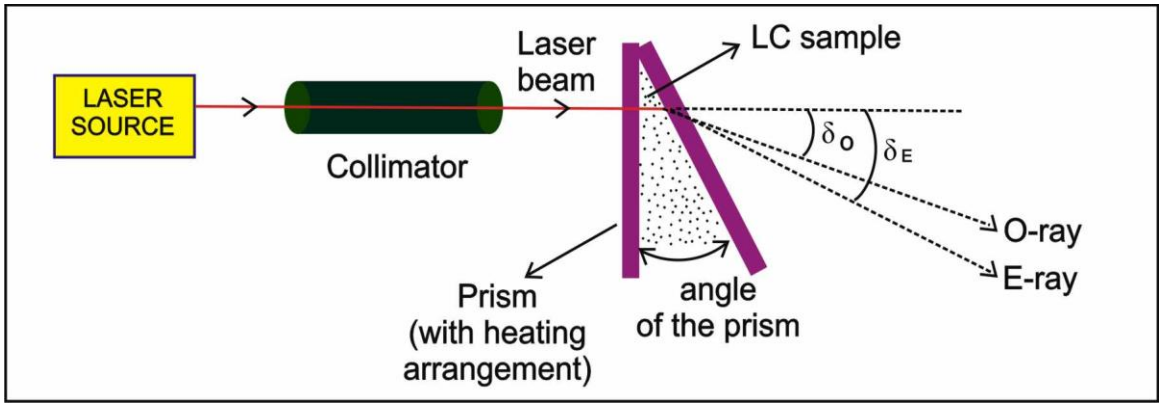

Figure 2.8: Schematic arrangement for the measurement of refractive indices

Measurement of Density

The density of the liquid crystalline samples were measured at different temperatures during both heating and cooling using a borosillicate glass tube dilatometer of capillary type, a travelling microscope and temperature controller. A weighed sample of the liquid crystal was introduced inside the dilatometer in isotropic state and was placed in a thermostated silica oil bath. The bulb of the dilatometer was filled with mercury. Sufficient time was allowed to reach the equilibrium at the desired temperature before taking each reading. The length of the liquid crystal column was measured at different temperatures with a travelling microscope .The densities were calculated after correction of glass expansion. Average value of the data obtained during heating and cooling are presented which are accurate within ±0.1%.

Calculation of Optical Polarizabilities from Refractive Index and Density Measurements

The molecular polarizability (α) of the molecules and order parameter control the optical anisotropy. The linear molecules having a long and rigid core exhibit high order parameter. Molecules that consist of high polarizability units (having π and delocalized electrons) such as aromatic rings in the core, tolane linking groups and terminal cyano groups have a high birefringence. Conversely, a low birefringence is exhibited by molecules that are deficient in these types of groups and usually consist of alicyclic groups and terminal alkyl chains. The molecular polarizability 'α' can be determined if the value of internal field, i.e., the average field acting on an individual molecule is known. Lorenz-Lorentz field, commonly known internal field valid for isotropic phase, is not applicable for mesogenic systems. Therefore, more realistic internal field, proposed by the Vuks' [51] and Neugebauer's [52] are usually applied in liquid crystalline systems.

Vuks' Method

Considering the internal field independent of molecular interaction, Vuks' derived the relations for polarizabilities associated with anisotropic molecules. In this case the effective molecular polarizabilities α_o and α_e, perpendicular and parallel to the direction of molecular axes, are related to n_o and n_e by the following equations

$$\alpha_o = \frac{3}{4\pi N}\frac{n_o^2 - 1}{n^2 + 2} \tag{2.22}$$

$$\alpha_e = \frac{3}{4\pi N}\frac{n_e^2 - 1}{n^2 + 2} \tag{2.23}$$

where N is the number of molecules per unit volume obtained from measured density and n is the mean refractive index and is given by

$$n^2 = \frac{1}{3}\left(2n_o^2 + n_e^2\right) \tag{2.24}$$

Neugebauer's Method

In this method internal field is calculated by representing the polarizability of a molecule by anisotropic point polarizability. Here the Lorenz-Lorentz equation for an isotropic system is extended to an anisotropic system. The relevant relations derived by Neugebauer are as follows:

$$n_e^2 - 1 = 4\pi N\alpha_e\left(1 - N\alpha_e\gamma_e\right)^{-1} \tag{2.25}$$

$$n_o^2 - 1 = 4\pi N\alpha_o\left(1 - N\alpha_o\gamma_o\right)^{-1} \tag{2.26}$$

where N is the number of molecules per unit volume and γ_e and γ_o are the respective internal field constants for extraordinary and ordinary rays. The equations necessary for calculating polarisabilities α_o and α_e obtained from the above equations are:

$$\frac{1}{\alpha_e} + \frac{2}{\alpha_o} = \frac{4\pi N}{3}\left[\frac{n_e^2 + 2}{n_e^2 - 1} + \frac{2\left(n_o^2 + 2\right)}{n_o^2 - 1}\right] \tag{2.27}$$

$$\alpha_e + 2\alpha_o = \frac{9}{4\pi N}\left[\frac{n^2 - 1}{n^2 + 2}\right] \tag{2.28}$$

Principal polarizabilities can be obtained by solving the above two equations.

Calculation of Orientational Order Parameter from Polarizability

The degree of order of the mesogenic molecule has been determined using polarizability values obtained from the above two methods. The principal polarizabilities, parallel and perpendicular to the direction of molecular axes, are related to the orientational order parameter [53-55] as

$$\alpha_e = \bar{\alpha} + \frac{2}{3}\Delta\alpha S$$

$$\alpha_o = \bar{\alpha} - \frac{1}{3}\Delta\alpha S$$

So, $$S = \langle P_2 \rangle = \frac{\alpha_e - \alpha_o}{\alpha_{\parallel} - \alpha_{\perp}} \qquad (2.29)$$

where $\bar{\alpha} = (2\alpha_o + \alpha_e)/3$, is the mean polarizability and $\Delta\alpha=\alpha_e-\alpha_o$ is the polarizability anisotropy. Here, S is the macroscopic order parameter and $\alpha_{\parallel}$ and $\alpha_{\perp}$ are the principal polarizabilities parallel and perpendicular to the long molecular axis in the perfectly ordered crystalline state where S=1. By using Haller's extrapolation procedure [56] one can get the values of $(\alpha_{\parallel}-\alpha_{\perp})$ in the solid state. In this method a graph is drawn by plotting log $(\alpha_e - \alpha_o)$ against log $(T_c - T)$ which should be a straight line. This line is extrapolated up to log (T_c), giving the value of $(\alpha_e - \alpha_o)_{T=0} = (\alpha_{\parallel} - \alpha_{\perp})$, T_c being the N-I transition temperature.

2.2.5 Dielectric Anisotropy

A material that does not conduct electricity but can essentially store the electric charges by means of polarization is called dielectric. The most common liquid crystal molecules are rod like and are axially symmetric about its long axis or the director **n**. The dielectric constant along the long molecular axis $(\varepsilon_{\parallel})$ and perpendicular axis $(\varepsilon_{\perp})$ are different. The difference between this two is called the dielectric anisotropy $(\Delta\varepsilon = \varepsilon_{\parallel} - \varepsilon_{\perp})$. Dielectric anisotropy is very important parameter because the threshold voltage (V_{th}) and other operational parameters of liquid crystal displays depend on the anisotropy of the permittivities [57]. The value of $\Delta\varepsilon$ may be positive or negative depending on the angle between the permanent dipole moment and the molecular axis. The larger the dielectric anisotropy value is for a liquid crystal molecule, the weaker the electric field must be to reorient the dipole moment along the field direction. The dielectric anisotropy of liquid crystals is inversely proportional to temperature. As the temperature reaches the clearing point of a liquid crystal, the dielectric anisotropy abruptly approaches zero. Dielectric permittivities of nematic liquid crystals have extensively been studied both experimentally and theoretically [58-61].

Maier and Meier Theory of Dielectrics for Liquid Crystals

W. Maier and G. Meier [62] extended the Onsager theory [63] of isotropic dielectrics to nematics to correlate the dielectric properties to molecular parameters. According to Maier and

Meier theory, nematics are composed of molecules with polarizabilities $\alpha_{\parallel}$, $\alpha_{\perp}$ and permanent dipole moment μ having components $\mu_{\parallel} = \mu\cos\theta$, $\mu_{\perp} = \mu\sin\theta$ along and perpendicular to molecular long axis. The molecule is considered to be in a spherical cavity surrounded by a continuum with macroscopic properties of the dielectric. The dielectric permittivities $\varepsilon_{\parallel}$ and $\varepsilon_{\perp}$ along and perpendicular to the molecular long axis in a static field are then given by

$$\varepsilon_{\parallel} = 1 + 4\pi NhF\left\{\bar{\alpha} + \frac{2}{3}\Delta\alpha S + F\frac{\langle\mu_{\parallel}^2\rangle}{kT}\right\} \tag{2.30}$$

$$\varepsilon_{\perp} = 1 + 4\pi NhF\left\{\bar{\alpha} - \frac{1}{3}\Delta\alpha S + F\frac{\langle\mu_{\perp}^2\rangle}{kT}\right\} \tag{2.31}$$

with $$\langle\mu_{\parallel}^2\rangle = \frac{\mu^2}{3}\left[1-(1-3\cos^2\theta)S\right]$$

$$\langle\mu_{\perp}^2\rangle = \frac{\mu^2}{3}\left[1+\frac{1}{2}(1-3\cos^2\theta)S\right]$$

Therefore, $$\Delta\varepsilon = \varepsilon_{\parallel} - \varepsilon_{\perp} = 4\pi NhF\left\{\Delta\alpha - F\frac{\mu^2}{2kT}(1-3\cos^2\theta)\right\}S \tag{2.32}$$

$$\bar{\varepsilon} = \frac{\varepsilon_{\parallel} + 2\varepsilon_{\perp}}{3} = 1 + 4\pi NhF\left\{\bar{\alpha} + F\frac{\mu^2}{3kT}\right\} \tag{2.33}$$

For isotropic phase (order parameter S=0), the permittivity becomes

$$\varepsilon_{iso} = 1 + 4\pi NhF\left\{\alpha_{iso} + F\frac{\mu^2}{3kT}\right\} \tag{2.34}$$

where N = the particle density = $\rho N_A/M$; ρ=mass density, N_A=Avogadro No., M=Molecular weight and $\bar{\alpha}$ = mean polarizability given by

$$\bar{\alpha} = \frac{\alpha_{\parallel} + 2\alpha_{\perp}}{3} \tag{2.35}$$

$\Delta\alpha$ = polarizability anisotropy = $\alpha_{\parallel} - \alpha_{\perp}$; h and F are respectively the cavity field factor and the reaction field factor and are given by

$$h = \frac{3\bar{\varepsilon}}{2\bar{\varepsilon}+1} \qquad \text{and} \qquad F = \frac{1}{(1-\alpha \bar{f})}$$

Here the factor f, called Onsager factor, is given by

$$f = \frac{8\pi}{3} N \frac{\bar{\varepsilon}-1}{2\bar{\varepsilon}+1}$$

The above equation 2.30 and 2.31 for $\varepsilon_{\parallel}$ and $\varepsilon_{\perp}$ are used to find effective dipole moment of the molecules in nematic phase and its orientation with molecular long axis. Alternatively, one may find the order parameter S when all remaining quantities are known. Maier-Maier's equations satisfactorily explain many essential features of the permittivity of liquid crystals consisting of polar molecules.

Dipole-Dipole Correlation Factor

The Onsager–Kirkwood– Fröhlich (OKF) equation occupies a central place in the study of liquid crystals because it allows the estimation of dipole-dipole correlation factor (g_λ) from measurable physical properties and thus to probe into the molecular organization of liquid crystals and their mixtures. In a liquid crystal constituted by polar molecules, the correlation factor expresses the deviation from randomness of the orientation of a dipole with respect to its neighbours. The ensemble averages of the parallel (||) and perpendicular (⊥) components of the molecular dipole moments are calculated following the procedure of Bata and Buka [64]. The dipole-dipole correlation factor (g_λ) can be expressed as

$$g_\lambda = \frac{\langle \sum_{i \neq j} (\mu_\lambda)_i (\mu_\lambda)_j \rangle}{\langle \mu_\lambda^2 \rangle} \qquad (2.36)$$

where the subscript λ refers to axes || and ⊥ to the nematic director.

Although the short-range dipole-dipole interactions are not considered in Maier-Meier theory [63], the Kirkwood-Fröhlich theory for isotropic liquid dielectrics [60,65] provides a formula in which these short-range effects are considered. Bordewijk and de Jeu [66-69] extended this idea to anisotropic media with uniaxial symmetry and used it to find dipole-dipole

correlation factor for nematic liquid crystals. Their model was based on experimentally observed proportionality between the square of birefringence (Δn^2) and the product of the density (ρ) and order parameter (S). Bata and Buka [64] later obtained the following relation between the low and high frequency dielectric permittivity components and the molecular parameters as

$$\varepsilon_\lambda - \varepsilon_{\infty\lambda} = \frac{4\pi N}{9kT}\frac{\varepsilon_\lambda(\varepsilon_{\infty\lambda}+2)^2}{(2\varepsilon_\lambda+\varepsilon_{\infty\lambda})}\left\langle\mu_\lambda^2\right\rangle f_\lambda(\varepsilon,\Omega_\lambda^\varepsilon)g_\lambda \tag{2.37}$$

where

$$f_\lambda(\varepsilon,\Omega_\lambda^\varepsilon) = \frac{2\varepsilon_\lambda+\varepsilon_{\infty\lambda}}{\varepsilon_\lambda-(\varepsilon_\lambda-\varepsilon_{\infty\lambda})\Omega_\lambda^\varepsilon} \tag{2.38}$$

Here $\Omega^{\varepsilon}_{\lambda}$ is a factor which depends on the dielectric anisotropy of the system. For positive dielectric anisotropy [67] one has

$$\Omega_{II}^\varepsilon = \frac{\varepsilon_{II}}{\varepsilon_{II}-\varepsilon_\perp} - \frac{\varepsilon_{II}.\varepsilon_\perp^{\frac{1}{2}}}{(\varepsilon_{II}-\varepsilon_\perp)^{3/2}}\tan^{-1}\left(\frac{\varepsilon_{II}-\varepsilon_\perp}{\varepsilon_\perp}\right)^{\frac{1}{2}} \tag{2.39}$$

and

$$\Omega_\perp^\varepsilon = \frac{\varepsilon_{II}\varepsilon_\perp^{\frac{1}{2}}}{2(\varepsilon_{II}-\varepsilon_\perp)^{3/2}}\tan^{-1}\left(\frac{\varepsilon_{II}-\varepsilon_\perp}{\varepsilon_\perp}\right)^{\frac{1}{2}} - \frac{\varepsilon_\perp}{2(\varepsilon_{II}-\varepsilon_\perp)} \tag{2.40}$$

For negative dielectric anisotropy

$$\Omega_{II}^\varepsilon = \frac{\varepsilon_{II}\varepsilon_\perp^{\frac{1}{2}}}{2(\varepsilon_\perp-\varepsilon_{II})^{3/2}}\left(\ln\frac{\varepsilon_\perp^{\frac{1}{2}}+(\varepsilon_\perp-\varepsilon_{II})^{\frac{1}{2}}}{\varepsilon_\perp^{\frac{1}{2}}-(\varepsilon_\perp-\varepsilon_{II})^{\frac{1}{2}}}\right) - \frac{\varepsilon_{II}}{\varepsilon_\perp-\varepsilon_{II}} \tag{2.41}$$

$$\Omega_\perp^\varepsilon = \frac{\varepsilon_\perp}{2(\varepsilon_\perp-\varepsilon_{II})} + \frac{\varepsilon_{II}\varepsilon_\perp^{\frac{1}{2}}}{4(\varepsilon_\perp-\varepsilon_{II})^{3/2}}\left(\ln\frac{\varepsilon_\perp^{\frac{1}{2}}-(\varepsilon_\perp-\varepsilon_{II})^{\frac{1}{2}}}{\varepsilon_\perp^{\frac{1}{2}}+(\varepsilon_\perp-\varepsilon_{II})^{\frac{1}{2}}}\right) \tag{2.42}$$

Therefore

$$\Omega_{\perp}^{\varepsilon} = \frac{1}{2}(1-\Omega_{\parallel}^{\varepsilon})$$

The average components of the effective dipole moment, $< \mu^2_{\parallel} >$ and $< \mu^2_{\perp} >$, appearing in equation (2.37) are evaluated as

$$\langle \mu_{\parallel}^2 \rangle = \frac{1}{3}\left\{(2S+1)\left[\frac{\varepsilon_{\infty\parallel}+(1-\varepsilon_{\infty\parallel})\Omega_{\parallel}^{sh}}{\varepsilon_{\infty\parallel}}\right]^2 \mu_{m\parallel}^2 + (1-S)\left[\frac{\varepsilon_{\infty\perp}+(1-\varepsilon_{\infty\perp})\Omega_{\perp}^{sh}}{\varepsilon_{\infty\perp}}\right]^2 \mu_{m\perp}^2\right\} \quad (2.43)$$

$$\langle \mu_{\perp}^2 \rangle = \frac{2}{3}\left\{(1-S)\left[\frac{\varepsilon_{\infty\parallel}+(1-\varepsilon_{\infty\parallel})\Omega_{\parallel}^{sh}}{\varepsilon_{\infty\parallel}}\right]^2 \mu_{m\parallel}^2 + \frac{1}{2}(S+2)\left[\frac{\varepsilon_{\infty\perp}+(1-\varepsilon_{\infty\perp})\Omega_{\perp}^{sh}}{\varepsilon_{\infty\perp}}\right]^2 \mu_{m\perp}^2\right\} \quad (2.44)$$

where the cavity field factor was calculated taking into account the following shape factors (Ω_{λ}^{sh}) of ellipsoidal molecules or prolate spheroid molecules with semi-long axis a and semi-short axis b.

$$\Omega_{\parallel}^{sh} = 1-\omega^2 + \frac{1}{2}\omega(\omega^2-1)\ln\frac{\omega+1}{\omega-1} \quad (2.45)$$

and

$$\Omega_{\perp}^{sh} = \frac{1}{2}\omega^2 - \frac{1}{4}\omega(\omega^2-1)\ln\frac{\omega+1}{\omega-1} \quad (2.46)$$

So,

$$\Omega_{\perp}^{sh} = \frac{1}{2}(1-\Omega_{\parallel}^{sh})$$

where $$\omega^2 = \frac{a^2}{a^2-b^2} \quad (2.47)$$

Taking apparent molecular length (l_{ap}) obtained from X-ray study as the value of 2a, b is calculated using the relation

$$b = \frac{1}{2}\left[\frac{6M}{\pi N_A l_{ap}\rho}\right]^{\frac{1}{2}} \tag{2.48}$$

on the assumption that the volume occupied by a molecule in the liquid crystalline phase is equal to the geometrical volume of the molecule [69]. They also used $\varepsilon_{\parallel\infty} = 1.05\, n_{\parallel}^2$ to take into account the atomic polarization factor. Since, according to Kirkwood and Fröhlich theory, the effective value of molecular dipole moment is given by:

$$\mu^2_{\text{eff}\,.\parallel} = \frac{9kT}{4\pi N}\frac{(\varepsilon_{\parallel} - \varepsilon_{\infty\parallel})(2\varepsilon_{\parallel} + \varepsilon_{\infty\parallel})}{\varepsilon_{\parallel}(\varepsilon_{\infty\parallel} + 2)^2} \tag{2.49}$$

So, with the help of equation (2.37) we can rewrite equation (2.49) as

$$\mu^2_{\text{eff}\ \parallel} = f_{\parallel}(\varepsilon, \Omega_{\parallel}) g_{\parallel}(\varepsilon, T_{\parallel}) \langle \mu^2_{\parallel} \rangle \tag{2.50}$$

So that

$$g_{\parallel} = \frac{\mu^2_{\text{eff}\,\parallel}}{f_{\parallel}\langle \mu^2_{\parallel} \rangle} \tag{2.51}$$

Similarly for the perpendicular component we have:

$$\mu^2_{\text{eff}\,.\perp} = \frac{9kT}{4\pi N}\frac{(\varepsilon_{\perp} - \varepsilon_{\infty\perp})(2\varepsilon_{\perp} + \varepsilon_{\infty\perp})}{\varepsilon_{\perp}(\varepsilon_{\infty\perp} + 2)^2} \tag{2.52}$$

and

$$g_{\perp} = \frac{\mu^2_{\text{eff}\,\perp}}{f_{\perp}\dfrac{\langle \mu^2_{\perp} \rangle}{2}} \tag{2.53}$$

where the factor 2 arises due to rotational symmetry. Equations 2.51 and 2.53 were used to calculate $g_{\parallel}$ and $g_{\perp}$. Further for a uniaxial liquid crystals de Jeu et al. [70,71] obtained the following equation for short range order parameter (T_{λ})

$$T_{\lambda} = (1 - g_{\lambda})\frac{kT}{4\pi N\langle \mu^2_{\lambda} \rangle} \tag{2.54}$$

2.2.6 Frequency Domain Dielectric Spectroscopy

Dielectric spectroscopy occupies an important role among numerous modern methods used for physical and chemical analysis of materials. By studying dielectric spectroscopy one can investigate the relaxation processes of complex systems over an extremely wide range of characteristic times. I have already discussed about the dielectric permittivity in static fields. When the field is removed the orientational polarization decays exponentially with a characteristic time τ called relaxation time. On reversing the field a definite time interval is required for reorientation of the permanent dipoles. In alternating fields this leads to a time lag between the average orientation of the dipole moments and fields. At much higher frequencies the orientation polarization can no longer follow the variation of the field and response of materials to alternating fields is characterized by a complex dielectric permittivity and is expressed as

$$\varepsilon^*(\omega) = \varepsilon'(\omega) - i\varepsilon''(\omega) \tag{2.55}$$

where $\varepsilon^{/}(\omega)$ is the real part of dielectric permittivity, which is related to the stored energy within the medium, and $\varepsilon^{//}(\omega)$ is the imaginary part of the permittivity and is related to the dissipation (or loss) of energy within the medium.

Debye and Cole-Cole Model

According to Debye, complex dielectric permittivity can be described in terms of a single relaxation time τ as follows:

$$\varepsilon^* = \varepsilon'(\omega) - i\varepsilon''(\omega) = \varepsilon_\infty + \frac{\varepsilon_0 - \varepsilon_\infty}{1 + i\omega\tau} \tag{2.56}$$

This is known as Debye equation [72]. ε_o and ε_∞ are the low and high frequency permittivities, ω is the angular frequency of the applied field and τ is the dielectric relaxation time related to the critical frequency (f_c) by the formula

$$\tau = \frac{1}{2\pi f_c} \tag{2.57}$$

Debye equation (2.56) can be separated into real and imaginary parts:

$$\varepsilon' = \varepsilon_\infty + \frac{\varepsilon_0 - \varepsilon_\infty}{1+(\omega\tau)^2} \tag{2.58}$$

$$\varepsilon'' = \frac{\varepsilon_0 - \varepsilon_\infty}{1+(\omega\tau)^2}\omega\tau \tag{2.59}$$

where the first equation (2.58) describes the dispersion process and the second equation (2.59) describes the absorption process. ε" reaches its maximum at critical frequency:

$$\varepsilon''(f) = \varepsilon''_{max} = \frac{\varepsilon_0 - \varepsilon_\infty}{2} \tag{2.60}$$

$\Delta\varepsilon = \varepsilon_o - \varepsilon_\infty$, is called the dielectric increment or strength. If one plots both the components of the dielectric permittivity versus frequency on the logarithmic scale one obtains typical dielectric spectrum as shown in the Figure 2.9. The curve which relates the frequency dependence of ε' is known as the dispersion curve whereas that of frequency dependence of ε" is called the absorption curve. The frequency at which ε" reaches its maximum is known as critical frequency (or relaxation frequency). Plot of ε" against ε' is known as Cole-Cole plot which for a Debye type liquid is a semi-circle.

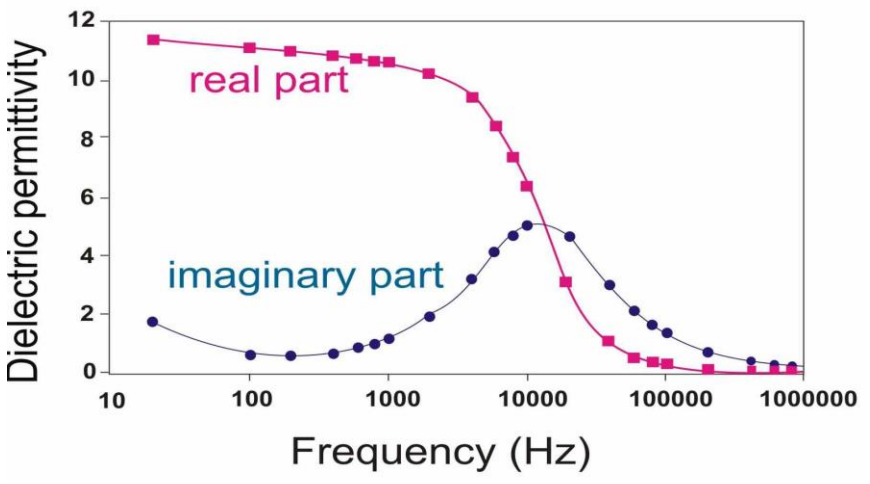

Figure 2.9: A typical dielectric sprectra for a Debye type liquid crystal

In case of paraelectric, ferroelectric, ferrielectric and antiferroelectric liquid crystals, dielectric spectroscopy detects stochastic reorientation of molecular dipole moments and

collective fluctuations of spontaneous polarization [72]. The dielectric spectrum for liquids and solid rotator phases of organic polar compounds [73-75] usually shows Debye-type behaviour. However, some systems composed of flexible molecules [74,76-78], some disordered solid phases [79-81] and achiral and chiral liquid crystals [72,82] that exhibit broad dielectric spectra cannot be described by Debye equation. In order to describe those systems, which do not relax with a single relaxation time, Cole and Cole [83] have extended the Debye equation by introducing the relaxation distribution parameter α as follows:

$$\varepsilon^* = \varepsilon' - i\varepsilon'' = \varepsilon_\infty + \frac{\varepsilon_0 - \varepsilon_\infty}{1 + (i\omega\tau_0)^{1-\alpha}} - i\frac{\sigma}{\omega\varepsilon_0} \tag{2.61}$$

which can be separated into two components:

$$\varepsilon'(\omega) = \varepsilon_\infty + \Delta\varepsilon \frac{1 + (\omega\tau_0)^{1-\alpha} \sin\left(\frac{1}{2}\pi\alpha\right)}{1 + 2(\omega\tau_0)^{1-\alpha} \sin\left(\frac{1}{2}\pi\alpha\right) + (\omega\tau_0)^{2(1-\alpha)}} \tag{2.62}$$

$$\varepsilon''(\omega) = \Delta\varepsilon \frac{1 + (\omega\tau_0)^{1-\alpha} \cos\left(\frac{1}{2}\pi\alpha\right)}{1 + 2(\omega\tau_0)^{1-\alpha} \sin\left(\frac{1}{2}\pi\alpha\right) + (\omega\tau_0)^{2(1-\alpha)}} + \frac{\sigma}{\omega\varepsilon_0} \tag{2.63}$$

Distribution parameter α varies from 0 to 1 which is responsible for symmetric distribution of the relaxation times. $\Delta\varepsilon = \varepsilon_o - \varepsilon_\infty$ is the dielectric strength, τ_0 is in this case the most probable relaxation time related to the critical frequency ($\omega_o\tau_o=1$). ε_o = 8.85 pFm^{-1} is the dielectric permittivity of the free space and σ is the conductivity. Here conductivity is related to the motion of charge carriers and is added to classical Cole-Cole function. The maximum value of $\varepsilon''(\omega)$ depends on the parameter α according to the formula:

$$\varepsilon''(\omega_c) = \varepsilon''_{max} = \frac{\varepsilon_0 - \varepsilon_\infty}{2} \frac{\cos\frac{\pi\alpha}{2}}{1 + \sin\frac{\pi\alpha}{2}} \tag{2.64}$$

For small values of the α parameter (α < 0.1) above equation takes the form:

$$\varepsilon''_{max} \cong \frac{\varepsilon_0 - \varepsilon_\infty}{2 + \alpha\pi} \qquad (2.65)$$

From the above relation it is clear that for the non-Debye dielectric relaxation processes the absorption peak is lower and broader as shown in the Figure 2.10. A more general function was proposed by Havriliak and Negami [74] which is more convenient to describe the relaxation of some disordered solids and also FLCs as well as AFLCs [84-90].

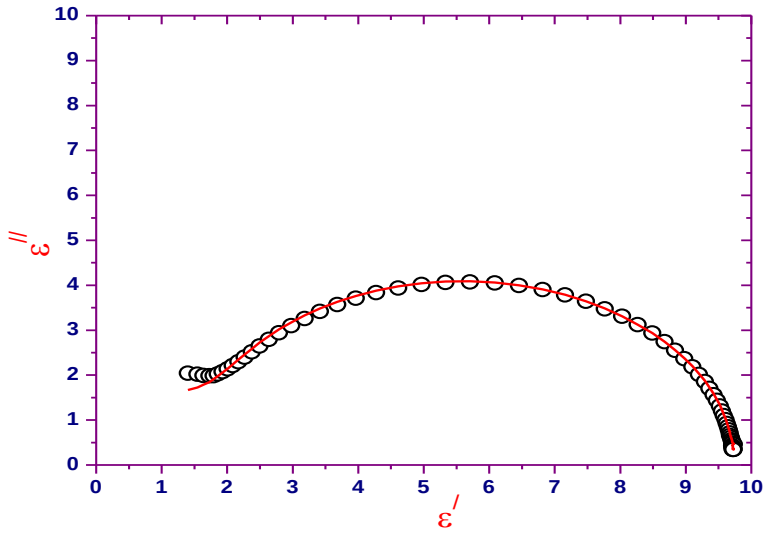

Figure 2.10: Cole-Cole plot for a Debye-type spectrum

Different Relaxation Processes in Chiral and Achiral Liquid Crystal Phases

There are basically two different types of relaxation processes in both chiral and achiral liquid crtstalline phase; viz. non-collective (molecular) and collective process. However, detection of the collective processes in the achiral phases is beyond the scope of dielectric relaxation measurement technique.

Non-Collective Processes

Non-collective processes can be observed in achiral and chiral systems i.e, molecules possessing nematic and smectic phases or possessing chiral smectic phases. There are four non-collective relaxation modes viz.

I] Molecular rotation around short axis.

II] Molecular rotation around long axis.

III] Intramolecular rotation around single bond.

IV] Motions of electrons relative to their nuclei.

In order to discuss the first two processes in nematic phase let us consider a molecule with a permanent dipole moment μ which makes an angle β with the long axis of a molecule shown in Figure 2.11. For nematic liquid crystal the order parameter always less than one, therefore each of the components of dipole moment, longitudinal and transverse to the long axis (μ_l and μ_t), should have a non zero projection both parallel and perpendicular to the director **n**, resulting in four relaxations, two in each measurement geometry, **E** $\parallel$ **n** and **E** $\perp$ **n**. But because of weak intensities of two absorptions related to μ_l and μ_t, we are left with two fundamental and characteristic absorptions of non-collective types in the chiral and achiral liquid crystal phases. The first one is observed in the homeotropic orientation and this molecular rotation is hindered by the nematic potential. The characteristic frequency is observed in the kHz and low MHz regime. The second process is observed in planar orientation and is not affected by the nematic potential and its characteristic frequency is observed in the high MHz and GHz regime as in normal liquids.

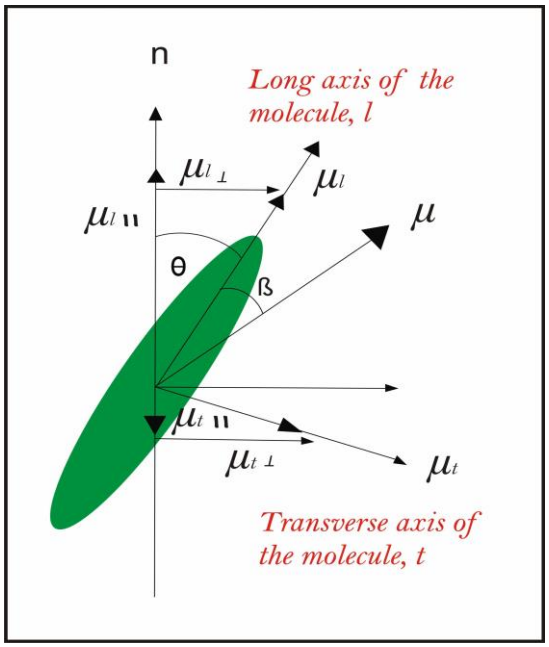

Figure 2.11: The molecular aspect of different dielectric absorption peaks

Collective Processes

In case of chiral smectic phases there are two additional collective absorption processes connected with the director fluctuation. These are

I] Soft mode (observed in SmA^* phase and near SmC^*- SmA^* transition)

II] Goldstone mode (observed in SmC^* phase)

The Goldstone mode (GM) and the soft mode (SM), has been examined by dielectric relaxation spectroscopy [91-94].

The Soft Mode

Soft mode relaxation arises due to the tilt angle fluctuation of the director. In SmA phase the molecules are aligned in the direction parallel to the layer normal and the stability of the structure is maintained by elastic constant. However due to thermal energy there may be some local instantaneous fluctuation of the tilt angle. Now if SmA phase is cooled down to SmA^*-SmC^* transition, the elastic constant controlling the tilt fluctuation gets soft. Thus the fluctuation amplitude increases drastically and consequently the phase will lose its stability and the

molecules fluctuate collectively like a group of drunken people. When a weak electric field is applied in a direction perpendicular to the director it can easily perturb the tilt fluctuation depending on how near the system is to the transition temperature. Thus the permittivity diverges and the frequency of tilt fluctuation falls to zero when the temperature approaches the transition temperature. In case of non-chiral SmA phase the amount of induced dipole moment due to the applied electric field is too small to be detected but for chiral SmA*, the chirality enhances the value of induced dipole moment due to the electroclinic effect which permits the soft mode study by dielectric measurement. In case of SmC* phase there exist a spontaneous tilt angle which grows from zero at transition and increases with decreasing temperature. Here also the molecules fluctuate collectively around the equilibrium tilt angle. Thus soft mode is present both in SmC and SmA phase. The characteristic frequency corresponding to soft mode is observed usually in the kHz regime.

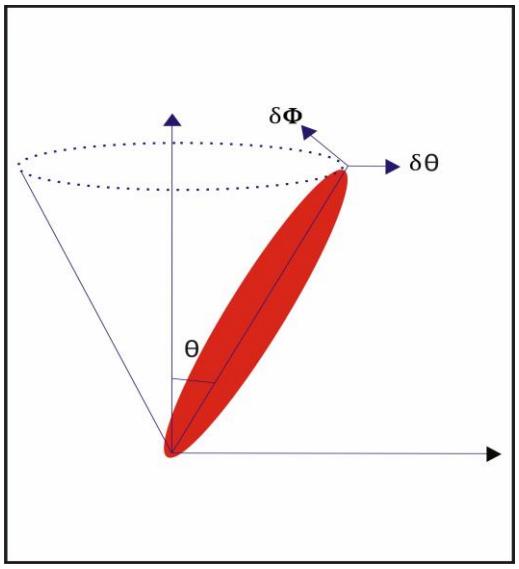

Figure 2.12: Molecular arrangement of tilt angle fluctuation and phase fluctuation

The Goldstone Mode

Beside tilt fluctuation, chiral SmC* phase possess phase fluctuation i.e, the molecules collectively oscillate around the smectic cone which gives rise to another collective relaxation, called the goldstone mode or phasor mode. The smectic C* phase has helical structure and molecular tilt. The director of smectic C* phase makes azimuthal angle φ with the smectic layer which changes from layer to layer resulting in a helical structure with helix axis parallel to the

smectic layer normal. Now if by thermal excitation the director in a certain layer fluctuate then that fluctuation will propagate along the helix axis which actually generates the phase fluctuation. The characteristic frequency corresponding to goldstone mode relaxation is observed normally in the frequency range between 10 Hz to 1 kHz. The GM dielectric increment ($\Delta\varepsilon_G$) is usually large compared to the SM increment ($\Delta\varepsilon_S$), so it is difficult to study the SM mode properties in the SmC* phase. Yet, this problem can be overcome by applying a DC bias field to the SmC* phase, the field should be strong enough to unwind the helical arrangement of the polarization vector. The SM can be studied almost separately by suppressing GM in this situation.

Dielectric Measurement Technique

To measure dielectric constant of a liquid crystalline sample, the ratio of capacitances of the filled and empty cell is to be found. For measuring the capacitances we employed an impedance analyzer (HP 4192A / HIOKI 3532-50) equipped with data acquisition system through RS232 interface. The temperature was controlled with a mettler hot stage (Mettler Toledo FP90) with an accuracy of ±0.1°C. The dielectric spectra were measured over the frequency range from 40 Hz to 5 MHz. Commercial cells (EHC/AWAT), of thickness few μm, were used in the form of a parallel plate capacitors made of indium tin oxide (ITO) coated glass plates which were pre-rubbed by polymer for achieving homogeneous (HG) alignment of the molecules. Cells were filled by capillary action with samples in isotropic state and cooled down to desired temperature very slowly to get homogenously aligned sample. By applying sufficient DC bias field homeotropic (HT) alignment of the molecules were achieved in the same cell. HG cell gives the $\varepsilon_\perp$ component when the measuring electric field was perpendicular to the nematic director and HT cell gives the $\varepsilon_\parallel$ component, measuring field being parallel to the director. On the other hand, custom built gold cells of thickness few μm and effective area 1.3 x 0.7 sq. cm were used for frequency dependent complex dielectric permittivity measurements. By AC capacitance bridge technique [95,96], the real and imaginary parts of the complex dielectric permittivity are obtained as a function of frequency at temperatures of interest. The experimental setup for dielectric permittivity measurement is shown in Figure 2.13.

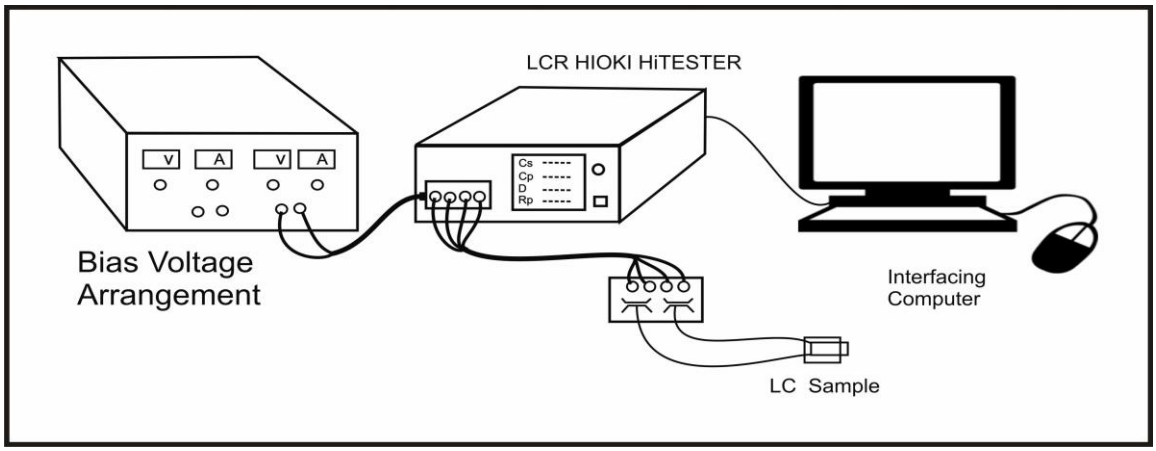

Figure 2.13: Schematic arrangement for the measurement of dielectric permittivity

2.2.7 Elastic Constants

The performances of liquid crystal display devices depend on the elastic properties of the liquid crystal. Liquid crystal molecules exhibit an elastic restoring force due to which if a system experiences an external force that perturbs it from an equilibrium position a restoring torque returns the system to its initial state. If the liquid crystal is deformed by electrical or magnetic forces so as to result in a splay deformation, a reactive elastic force will tend to restore the initial configuration and the reactive forces is described by splay elastic constant (K_{11}). The same phenomenon will occur for a twist deformation as well as for a bend deformation and the respective constants are called twist elastic constant (K_{22}) and bend elastic constant (K_{33}). The three types of director deformations are shown in Figure 2.14. As a liquid crystal medium prefers a uniform director distribution, a variation of the director in space induces an increase of the free energy. According to the elastic theory for liquid crystals, the distortion energy can be expressed as

$$f_d = \frac{1}{2}\left[k_{11}\left(\nabla.\bar{n}\right)^2 + k_{22}\left(\bar{n}.\nabla\times\bar{n}\right)^2 + k_{33}\left(\bar{n}\times\nabla\times\bar{n}\right)^2\right] \qquad (2.66)$$

This equation is known as the Oseen-Frank distortion energy [97]. For most liquid crystal compounds, the three elastic constants have the following relationship: $K_{33}>K_{11}>K_{22}$.

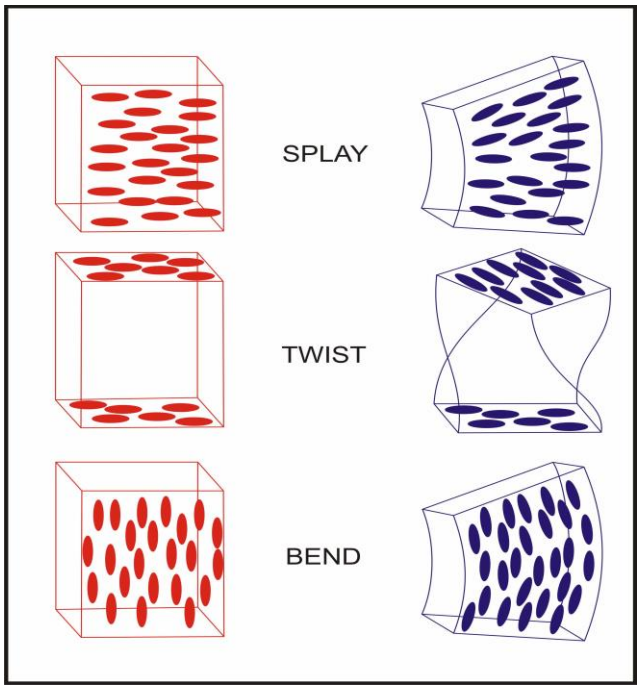

Figure 2.14: Molecular configuration of Splay, Twist and Bend elastic constants

Determination of Elastic Constants: Freedericksz Transition

The elastic constants are measured by the Freédericksz transition technique [98] where, an external electric or magnetic field is applied to deform the thin layer of surface aligned nematic liquid crystal having a uniform director (**n**) pattern. For a nematic liquid crystal with positive dielectric anisotropy ($\Delta\varepsilon > 0$), the determination of the elastic constants by threshold measurements requires a liquid-crystal cell made of two conducting glass plates with the director oriented parallel to the surface before the application of the field. Below the critical field the molecules remains surface aligned and above it the molecules align along the direction of the field. This phenomenon is known as Freedericksz transition. From the geometry of arrangement, the splay, twist and bend elastic constants can be determined from Freedericksz transition in a magnetic field. After application of an external electric field the dielectric energy is decreased by a tilting of the director and the total bulk free energy per unit area of the cell is given by [99]

$$G = \frac{1}{2}\int_0^L \{(K_{11}\cos^2\phi + K_{33}\sin^2\phi)(\frac{d\phi}{dz})^2 - E.D\}dz \qquad (2.67)$$

where Φ(z) is the tilt angle which is a function of the coordinate z along the cell thickness *L*. The first and second terms in the integrand are the elastic and dielectric energy densities and **E** and **D** are the electric and displacement fields respectively. The tilt angle is related to applied voltage V by [99]

$$\frac{V}{V_{th}} = \frac{2}{\pi}\sqrt{1+\gamma \sin^2 \phi_m}\int_0^{\frac{\pi}{2}}[\frac{(1+k\sin^2\phi_m \sin^2\psi)}{F(\psi)}]^{\frac{1}{2}} d\psi \qquad (2.68)$$

where

$$F(\psi) = (1+\gamma \sin^2 \phi_m \sin^2 \psi)(1-\sin^2 \phi_m \sin^2 \psi),$$

$$k = (K_{33} - K_{11})/K_{11},\ \gamma = (\varepsilon_{\mathrm{II}} - \varepsilon_{\perp})/\varepsilon_{\perp}$$

and

$$V_{th} = \pi\sqrt{\frac{K_{11}}{\varepsilon_0 \Delta\varepsilon}} \qquad (2.69)$$

is the Freédericksz threshold voltage, ε_0 is the dielectric constant of vacuum. The maximum distorted angle at the centre is $\Phi\ (L/2) = \Phi_m$, where $d\Phi/dz = 0$. For the twisted planar geometry

$$V_{th} = \pi\sqrt{\frac{1}{\varepsilon_0 \Delta\varepsilon}[K_{11} + \frac{K_{33} - 2K_{22}}{4}]} \qquad (2.70)$$

Thus by measuring Freédericksz threshold voltage and dielectric anisotropy, it is possible to find splay elastic constant K_{11} using equation 2.69. As switching time is inversely related to the elastic constant, a smaller value would result in a system that takes a longer amount of time to return to its equilibrium state which suggests the proper balance between response time and driving voltage is necessary for a better display application.

2.2.8 Measurement of Tilt Angle

Tilt angle is considered as the primary order parameter of ferroelectric SmC* phase which reflects the angle between the direction of molecular long axis and the layer normal. There are two ways to measure the tilt, one is optical method and another one is x-ray method. In a ferroelectric liquid crystal sample, on application of an external field, molecular director is switched by an angle 2θ (θ being the tilt angle of the material) in the plane of the substrates in SSFLC geometry as discussed in chapter 1. To get the tilt angle θ, first a homogeneously aligned FLC cell is mounted on the polarizing microscope. The polarizer and analyzer of the microscope are set in a crossed position. An electric field in the form of a square wave of very low frequency 0.1 Hz is applied to the sample so that molecules in the whole sample are aligned uniformly with a tilt θ away from the layer normal. The sample is rotated on a microscope table to get minima in optical transmission. When the field is reversed the molecules rotate along the tilt cone so that the final tilt becomes -θ from the layer normal. One has to rotate the sample stage until the previous minima (normally black) is obtained. The angle by which the microscope table was rotated from one minimum position to other minimum will be twice the tilt angle (2θ). One can measure it as a function of temperature.

Tilt angle can also be determined from X-ray study. To get the tilt angle one has to measure the layer spacing (d) by analyzing x-ray photographs and then by using the relation $\theta = \cos^{-1}(d/L)$, tilt angle can be evaluated, where L is the most extended length of the molecule found by geometry optimization. Often layer spacing in smectic A (d_A) phase is used instead of L.

2.2.9 Spontaneous Polarization

Ferroelectric liquid crystals possess non-enantiomorphic polar symmetry in their structures giving rise to a polarization that exists within a material in the absence of the application of an external field which called spontaneous polarization (P_S). In ferroelectric liquid crystals spontaneous polarization is treated as the secondary order parameter, since it is a result of the tilt of the molecules which is called the primary order parameter. The response time or

switching time (τ) of an FLC device is the most significant parameter and it is related to the spontaneous polarization as given by [100]

$$\tau = \frac{\gamma \sin \theta}{P_S E} \qquad (2.71)$$

where γ is rotational viscosity, θ is tilt angle and E is the applied electric field. Thus to achieve faster switching speed, τ should be as low as possible. For a portable device of low power consumption applied field E as well as viscosity γ and tilt angle θ should be low and P_S should be high. But a high value of P_S causes a current flow through the cell, which is undesirable. So a moderate level of P_S is required for a short switching time.

Measurements of Spontaneous Polarization by Triangular Wave Method

There are number of methods to measure the magnitude of P_S. One of the standard methods to know the ferroelectric behaviour is the Tower-Sawyer technique [101]. Other useful methods are reverse current method [102,103], reverse field method [104], electric-field dependent dielectric constant and pyroelectric method [105]. We have used the reverse current method using a triangular wave to calculate the spontaneous polarization (P_S). The experimental set up for this purpose is shown in Figure 2.15. As depicted in the figure a high resistance R (10, 100 or 1000 kΩ) is connected in series with the cell and output voltage across the standered resistance R is fed to the oscilloscope (Tektronix TDS 2012B). A 10 Hz, 20Vpp triangular signal was used from HP 34401A function generator, amplified by F20A Voltage amplifier for the purpose.

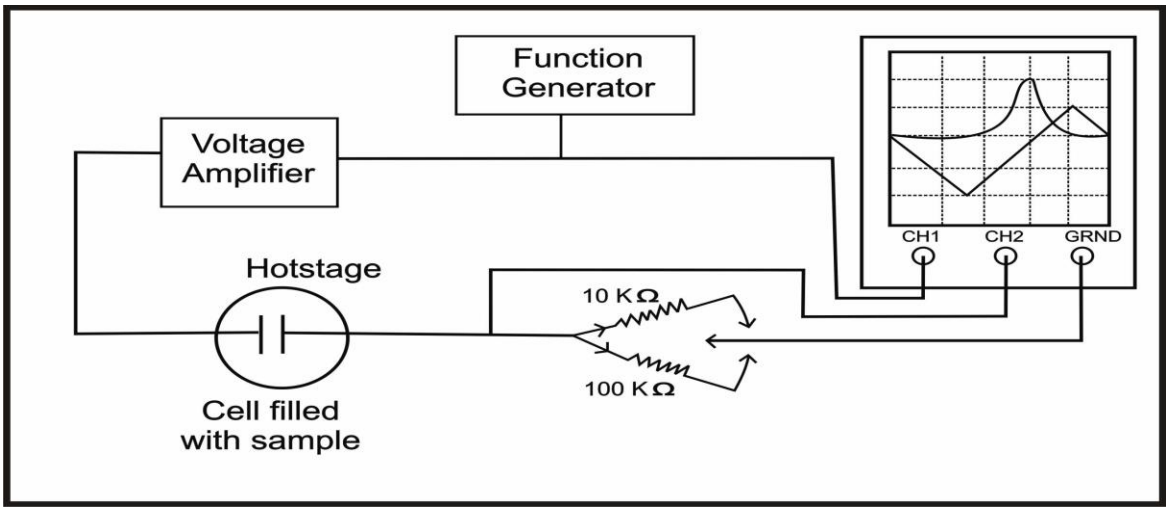

Figure 2.15: Experimental set up to measure the value of P_S

Current I(t) induced in the ferroelectric LC cell by applying a voltage V(t) can be written as a sum of the following three contributions:

$$I = Ic + Ip + Ii = C\left(\frac{dV}{dt}\right) + \frac{dP}{dt} + \frac{V}{R'} \qquad (2.72)$$

where Ic is charge accumulation in the capacitor (displacement current), Ip is the polarization realignment current and Ii is the ionic current R' is the effective resistance of the circuit. By selecting a suitable value of resistance R one can get suitable overall current profile to subtract the ionic and capacitive currents by drawing a baseline. The polarization current peaks appear on the oscilloscope due to polarization reversal and the area under the peaks gives direct estimate of P_s [106].

$$P_S = \frac{\int Vdt}{2AR} \qquad (2.73)$$

where R is the resistance used to record the V-t curve and A is the effective area of the cell used. Area under the curve was determined from the stored image after creating appropriate base line using Origin 7 software.

2.2.10 Measurement of Response Time: Electrical method

Response time is one of the most critical issues for nearly all liquid crystal (LC) devices involving dynamic switching. Response time in SSFLC depends on cell thickness, field strength, surface anchoring etc. as well as on material parameters like polarization, tilt angle and rotational viscosity [107]. Response time contains rise time and decay time. To quantify a display device, rise time and decay time is usually defined as intensity change between 10% and 90%. Response time can be measured either by monitoring electrical response to an applied square wave [108,109] or by using optical method [110].

The response time was studied in a setup similar to that used for spontaneous polarization measurement. In this case, instead of a triangular wave, a square wave signal is applied to FLC sample in SSFLC geometry and the current response associated with switching process is monitored as voltage across a series resistance in storage oscilloscope [109]. Polarization bump occurs away on the time scale from square pulse edge of the applied voltage, delay in time is caused by the response time of the FLC sample. Thus the time delay on the occurrence of the polarization bump from the applied square pulse edge directly gives response time of FLC sample.

2.2.11 Rotational Viscosity

Rotational viscosity (γ_Φ), which is related to rotations of the molecular directors about the smectic C^* cone, is another important parameters of the SmC* phase and strongly influences the switching time between the field-induced states of FLCs. So, rotational viscosity plays a critical role to LC dynamics. Both the rise time and decay time are linearly proportional to γ_Φ. Thus, for most LC devices, low rotational viscosity material is favorable as evident from equation 2.71.

Measurement of Coefficient of Rotational Viscosity

The rotational viscosity in Goldstone mode was determined using the following relation derived from generalized Landau model [111]:

$$\gamma_{\phi} = \frac{1}{4\Pi\varepsilon_0} \cdot \frac{1}{\Delta\varepsilon f_c} \left(\frac{P_S}{\theta} \right)^2 \qquad (2.74)$$

where Goldstone mode dielectric strength (Δε) and relaxation frequency (f_C) were obtained from dielectric relaxation study and tilt angle (θ) was obtained from optical or X-ray techniques. From the molecular standpoint, the rotational viscosity depends on the molecular constituents, dimensions, molecular interactions and moment of inertia.

2.2.12 Theory of Crystal Structure Determination

Since molecular order in liquid crystals is intermediate between that in liquid and crystalline state, molecular conformation and arrangement in the crystalline state often found to predetermine the molecular organization in the mesomorphic state. Bernal and Crowfoot [112] in the early 1930's, made the first attempt to correlate the molecular arrangement in the mesomorphic state with the crystal structure of the mesogenic material. However, after that a very few studies had been made for many years in the crystal structure determination. In the late 70's, due to the introduction of computer programs for solving structures a large number of structures of liquid crystal forming compounds have been determined which are mostly nematogens [113-127]. A detailed review on mesophase structure-property relationship was first given by Bryan [128] in early eighties and later by Haase and Athanassopoulou [129] in 1999. Crystal structures of a number of mesogenic compounds had also been reported from our laboratory in order to investigate the structure-property relationship [113-121, 130-133].

In a crystal the constituent atoms or molecules are arranged in a regular and periodic manner and they possess long range positional as well as orientational order. A unit cell of such arrangement can be constructed by three non coplanar vectors **a, b, c** along the three edges where α, β, and γ are the angles between the edges. When X-rays are scattered by the electrons of the

atoms the 2-D diffraction photographs so obtained contains features where intensity varies as a function of position. To locate the positions of the individual atoms in the unit cell, the intensity of the diffracted pattern must be measured and analyzed. If f_j be the amplitude scattered by the j-th atom at point $\mathbf{r}_j$ and if there are N such atoms within the cell, then the amplitude of the radiation scattered from the array of planes represented by the Miller indices (hkl) is given by [134],

$$F_{hkl} = \sum_{j=1}^{N} f_j \exp 2\pi i\left(hx_j + ky_j + lz_j\right) \tag{2.75}$$

where, f_j is called atomic scattering factor or form factor, F_{hkl} is known as the structure factor for the reflection hkl. $|F_{hkl}|$ is called the structure amplitude, a pure number- number of electrons. The above equation may also be written as

$$\mathbf{F_H} = \sum_{j=1}^{N} f_j \exp\left(2\pi i\mathbf{H}.\mathbf{r}_j\right) \tag{2.76}$$

where the reciprocal lattice vector has been replaced by **H**. As the atoms in the unit cell are at the positions of high electron density $\rho(\mathbf{r})$, so $F_{\mathbf{H}}$ can be expressed as

$$\mathbf{F_H} = \int_V \rho(r) \exp(2\pi i \mathrm{H}.r) dV \tag{2.77}$$

where V is the volume of the unit cell. The electron density ρ (**r**) can be represented as a Fourier series in three dimensions with structure factors as the Fourier coefficients

$$\rho(\mathbf{r}) = \frac{1}{V}\sum_h \sum_k \sum_l F_{\mathbf{H}} \exp\left(-2\pi i\mathbf{H}.\mathbf{r}\right) \tag{2.78}$$

Now by Fourier summation with a large number of $F_{\mathbf{H}}$ obtained from diffraction experiment, one can derive the crystal structure directly. However, from diffraction experiments one gets a set of diffraction intensities ($I_{\mathbf{H}}$) from different hkl planes which helps to get the magnitude of the structure factors $|F_{\mathbf{H}}|$, but not their phases $\phi_{\mathbf{H}}$ and this is the well-known *Phase Problem* in crystallography. To overcome this problem, we generally take help of four main methods viz., Patterson method, Direct methods, Isomorphous replacement technique and Anomalous scattering method. Only the direct methods [135] have been discussed briefly, since the structure of a liquid crystalline compound has been determined by this method.

Direct Methods

Direct methods try to evaluate the phases $\phi_{\mathbf{H}}$ directly from the observed intensities (I_{obs}) through probabilistic calculations. The direct methods are very efficient in solving crystal structures especially of low molecular weight organic compounds following the pioneering work of Herbert Hauptman and Jerome Karle for which they were awarded Novel prize in chemistry in 1985. Different computer programs are now available for solving crystal structures by direct methods viz., MULTAN [136], SIMPEL [137], SHELX[138], XTAL [139], SIR 92 [140], NRCVAX [141], SAPI [142], MITHRIL [143] etc.

A systematic account of the detail theory of direct methods is beyond the scope of this thesis. Only the basic principles and working formulae will be discussed here.

Structure Invariant and Seminvariants

A structure invariant is defined as a quantity that is independent of the shift of the origin of the unit cell. A simple example is that the intensities $I_{\mathbf{H}}$ of reflections i.e. $|F_{\mathbf{H}}|^2$ are structure invariants. However the structure factor itself is not structure invariant, otherwise the phase problem would not have occured. This is because, for any shift in the origin by, say, $\Delta\mathbf{r}$ the phase of $F_{\mathbf{H}}$ changes by $-2\pi\mathbf{H}.\Delta\mathbf{r}$ radians while the amplitude remains invariant. However, although individual phases depend on the structure and choice of origin, some combinations of them is structure invariant. For example, if $\mathbf{H}_1+\mathbf{H}_2+\mathbf{H}_3=0$ then $\phi_{\mathbf{H}1}+\phi_{\mathbf{H}2}+\phi_{\mathbf{H}3}$ is structure invariant for every space group. It follows directly from the fact that the product $F_{-\mathbf{H}}F_{\mathbf{K}}F_{\mathbf{H}-\mathbf{K}}$ is an invariant. Since the moduli of the structure factors are invariant themselves, the angular part of $F_{-\mathbf{H}}F_{\mathbf{K}}F_{\mathbf{H}-\mathbf{K}}$ is also invariant i.e. $\phi_{-\mathbf{H}} + \phi_{\mathbf{K}} + \phi_{\mathbf{H}-\mathbf{K}} = \phi(\mathbf{H},\mathbf{K}) = \phi_3$ is invariant. The value of a structure invariant is not, however, always known, even though it can only be a function of other structure invariants, e.g., intensities.

The structure seminvariants are those linear combinations of the phases whose values are uniquely determined by the crystal structure i.e., they do not change value on transfer from one special origin to another. It originates from space group symmetry. For example in space group $P\bar{1}$, the linear combination $2\phi_{-\mathbf{H}} + \phi_{2\mathbf{H}}$ is a structure invariant for any reciprocal vector **H.** For each space group they have to be derived separately. In any space group any structure invariant is

also a structure seminvariant, but reverse is always not true. A complete theory is given in a series of papers by Hauptman and Karle [144-146] and by Schenk [147].

Structure Determination Procedures

In order to solve the crystal structure a set of intensity data is required which is collected from the single crystal by computer-controlled CAD4 X-ray diffractometer using usually CuK_α/MoK_α radiation. The intensity data are corrected for Lorentz polarization factors [148]. The intensities are converted into the structure factors on an absolute scale by determining the scale factor by the method introduced by A. J. C Wilson [149]. A temperature factor is also obtained during the process that takes into account the thermal vibrations of the real atoms. After that the following steps are taken:

I] Estimation of normalised structure factors |E|'s from $|F_{obs}|$ values

II] Set up of phase relationships via structure invariants and seminvariants, starting phase determination, phase extension and refinement

III] Calculation of figure of merit of different phase sets

IV] Production of E-map by Fourier method and their interpretation

V] Refinement of structures through Fourier synthesis, Difference Fourier synthesis and Least-squares refinement techniques.

I] Estimation of $|E|$'s from $|F_{obs}|$ values

In direct methods, since the phases of the structure factors are estimated directly from the structure amplitudes so it becomes necessary that the structure amplitudes be judged on their intrinsic merit where the decrease of the atomic scattering factor with increasing scattering angle has to be eliminated. As the amplitudes of the different structure factors, $F_{\mathbf{H}}$, cannot be compared directly, since the scattering factor decreases with increasing reflection angle θ, the observed $|F_{\mathbf{H}}|$ is therefore modified so that they correspond to the hypothetical diffracted waves which would be obtained if atoms were stationary point atoms. The modified structure factor, called 'Normalised structure factor' ($E_{\mathbf{H}}$**),** is defined as,

$$\left|E_{\mathbf{H}}\right|^2 = \frac{I_h}{\langle I \rangle} = \frac{\left|F_{\mathbf{H}}\right|^2}{\varepsilon \sum_{j=1}^{N} f_j^2}$$

where ε is an integer characteristic of the space group symmetry.

II] Setting up of phase relationships, starting phase determination, phase extension and refinement

At the beginning, phases of strong reflections are determined. In practice 10 reflections per atom in the asymmetric unit seem quite satisfactory and in some cases as few as three to five per atom have served. If the crystal is triclinic or non-centrosymmetric; more reflections may be required.

The most commonly used phase relation is a three phase structure invariants based on the positivity of electron density criterion, as proposed by Karle and Karle [146]:

$$\phi_{\mathbf{H}} \approx \phi_{\mathbf{K}} + \phi_{\mathbf{H}-\mathbf{K}} \qquad (2.79)$$

which for centrosymmetric structure is expressed by signs as

$$S(H) \approx S(K)\, S(H - K) \qquad (2.80)$$

Relation (2.79) is used to generate phases $\phi_{\mathbf{H}}$ when the values of the phases on the right-hand side are known and it is used in a cyclic manner to propagate the phases to all the selected reflections. These relations are probability relations and the probability is high when the reflections have large |E| values in addition to satisfying the criterion H + K + L = 0. These are called Σ_2 phase relations. Probability of the phase of H being equal to the sum of the phases of – H and H-K is given by the following relations. In centrosymmetric case [150]:

$$P_+(\mathbf{H}, \mathbf{K}) = \frac{1}{2} + \frac{1}{2} \tanh\left[\frac{1}{2} k(\mathbf{H}, \mathbf{K})\right] \qquad (2.81)$$

In non-centrosymmetric case [151]:

$$P[\phi(\mathbf{H},\mathbf{K})] = \frac{\exp\{k(\mathbf{H},\mathbf{K})\cos[\phi(\mathbf{H},\mathbf{K})]\}}{2\pi I_o\{k(\mathbf{H},\mathbf{K})\}} \tag{2.82}$$

where I_o is a zero-order modified Bessel function of the first kind.

Now the question arises about deciding the phase of a particular reflection when there are several pairs of known phases, the estimate from each of which might be well different. The answer to this important problem was given by Karle and Hauptman [152] in 1956. They introduced the tangent formula

$$\tan\phi_{\mathbf{H}} \approx \frac{\sum_{\mathbf{K}} k(\mathbf{H},\mathbf{K})\sin(\phi_{\mathbf{K}} + \phi_{\mathbf{H}-\mathbf{K}})}{\sum_{\mathbf{K}} k(\mathbf{H},\mathbf{K})\cos(\phi_{\mathbf{K}} + \phi_{\mathbf{H}-\mathbf{K}})} = \frac{B(\mathbf{H})}{A(\mathbf{H})} \tag{2.83}$$

where $$k(\mathbf{H},\mathbf{K}) = 2\sigma_3\sigma_2^{-\frac{3}{2}}|E_{\mathbf{H}}||E_{\mathbf{K}}||E_{\mathbf{H}-\mathbf{K}}|$$

$$\sigma_n = \sum_{j=1}^{N} Z_j^n$$

Z_j being the atomic number of the j^{th} atom in a unit cell containing a total of N atoms. For identical atoms $\sigma_3\sigma_2^{-\frac{3}{2}} = N^{-\frac{1}{2}}$.

In order to use the tangent formula to obtain a new phase, the values of some phases have to be known and put into the right -hand side of the tangent formula. The set of the known phases is called a starting set from which the tangent formula derives more and more new phases and refines them in a self-consistent manner. But in this way all phases cannot be determined with acceptable reliability. It is therefore useful at this stage to eliminate about 10% of these reflections whose phases are most poorly defined by the tangent formula (2.83). An estimate of the reliability of each phase is obtained from $\alpha(\mathbf{H})$:

$$\alpha(\mathbf{H}) = \left\{A(\mathbf{H})^2 + B(\mathbf{H})^2\right\}^{\frac{1}{2}} \tag{2.84}$$

When the relation (2.84) contains only one term, as it may in the initial stages of the phase determination, then $\alpha(\mathbf{H}) = k(\mathbf{H},\mathbf{K})$.

The larger the value of $\alpha(\mathbf{H})$, the more the reliable is the phase estimate. The relation between $\alpha(\mathbf{H})$ and the variance is given by Karle and Karle [146], in 1966, as

$$\sigma^2(\mathbf{H}) = \frac{\pi^2}{3} + 4\sum_{t=1}^{\infty} \frac{(-1)^t}{t^2} \frac{I_t\{\alpha(\mathbf{H})\}}{I_0\{\alpha(\mathbf{H})\}}$$

From (2.88) it can be seen that $\alpha(\mathbf{H})$ can only be calculated when the phases are known. However, an estimate of $\alpha(\mathbf{H})$ can be obtained from the known distribution of three phase structure invariants [151]. The estimated $\alpha(\mathbf{H})$ at the initial stage is given approximately by

$$\alpha_{est}(\mathbf{H}) = \sum_{\mathbf{K}} k(\mathbf{H},\mathbf{K}) \frac{I_1\{k(\mathbf{H},\mathbf{K})\}}{I_0\{k(\mathbf{H},\mathbf{K})\}} \qquad (2.85)$$

The first step in phase extension is to fix the origin and enantiomorphs as the tangent phasing process is usually initiated with a few 'known' phases. This is done by imposing the condition in terms of structure factor seminvariant phases. The selection of starting phases is critical to the success of the multisolution methods. To maximize the connection between starting phases, the generator reflections are sorted by a convergence-type process by Germain, Main and Woolfson [136]. At the end of the convergence procedure a number of reflections, sufficient to fix the origin and the enantiomorphs whose phases are known, are obtained. A few other reflections are also chosen to which different phase values are assigned (either numerically or symbolically) to create different starting points for phase extension through Σ_2 relations. The strength of convergence procedure is that it ensures, as far as possible, that the initial phases will develop through strong and reliable phase relationships. For each starting phase set, phases of all the selected strong reflections are generated and refined as explained in earlier section. Thus we get a multiple phase sets.

III] Calculation of figure of merit of the generated phase sets

When a number of sets of phases have been developed, it is necessary to rank them according to some Figure-of-Merit (FOM), prior to computing a Fourier map (in this case E-map). Combining all weights from various FOM viz., Absolute Figure-of-Merit (ABSFOM), Relative Figure-of-Merit (RFOM), R-factor Figure-of-Merit (RFAC), Psi (zero) Figure-of-Merit (PSIO) etc. Combined Figure-of-Merit (CFOM) is calculated for each set. The most likely correct sets of phases are those with the highest value of CFOMs.

IV] E-map calculation and interpretation

Using the best phase set, E-maps are calculated using equation 2.78 at a large number of grid points covering the entire unit cell. The complete interpretation of the maps is done in three stages: peak search, separation of peaks into potentially bonded clusters and application of simple stereochemical criteria to identify possible molecular fragments. The molecular fragments thus obtained can be compared with the expected molecular structure. The computer can thus present the user with a list of peaks and their interpretation in terms of the expected molecular structure quite automatically. It is also common practice to have an output of the picture of the molecule as an easy check on the structure the computer has found.

V] Refinement of structures

Generally we use following three methods, viz., 1) Fourier synthesis, 2) Difference Fourier synthesis and 3) Least squares refinement [153,154] for refinement of a model structure (partial or complete) obtained from E-map. The Fourier synthesis gives the refined co-ordinates of the atoms and also tends to reveal the position of any atom that is not included in computing the structure factors using equation (2.75). The Difference Fourier map is very useful for correcting the position of an atom used in structure factor calculation. This is also very useful in locating H-atoms towards the final stages of refinement procedure.

An analytical method of refinement of great power and generality is that based on the principle of least squares. In brief, least-squares refinement consists in using the squares of the differences between observed and calculated structure factors as a measure of their disagreement and adjusting the parameters so that the total disagreement is a minimum.

The degree of refinement is indicated by an agreement between the calculated structures factors F_c and those observed, F_o. The most common method of assessing the agreement is calculating the residual or reliability index of the form

$$R = \frac{\sum\left(|F_o| - |F_c|\right)}{\sum|F_o|} \qquad (2.86)$$

the summation being over all the reflections. Evidently, the lower the value of R, the better is the agreement. Another form of the residual of common use is

$$R_w = \left[\frac{\sum w\left(\left|F_o - F_c\right|^2\right)}{\sum w\left|F_o\right|^2} \right]^{\frac{1}{2}} \tag{2.87}$$

where the frequently used weight is,

$$w = \frac{1}{\sigma^2\left(F_o\right)}$$

$\sigma(F_o)$ being the standard deviation of F_o. Using standard techniques, various parameters like bond lengths, bond angles, torsion angles, non bonded distance etc., are determined by determining the structure with a reasonably low R-value.

2.3 REFERENCES

[1] M. Born; Sitzb. kgl. preub. Akad. Wiss., 614 (1916), Theorie der flussigen Kristalle und des electrischen Kerr Effects in Flussigkeiten.

[2] P. G. de Gennes; The Physics of Liquid Crystals, Clarendon Press, Oxford (1974); P. G. de Gennes and J. Prost, 2nd ed. Clarendon Press, Oxford (1993).

[3] A. L. Tsykalo; Thermophysical properties of liquid crystals, Gordon and Breach Science Publishers, (1991).

[4] S. Chandrasekhar, Liquid Crystals, 2nd Edn., Cambridge University Press, Cambridge, (1992).

[5] I. Musevic, R. Blinc and B. Zeks's, The Phases of Ferroelectric and Antiferroelectric Liquid Crystals, World Scientific, Singapore (2000).

[6] W. Maier and A. Saupe, Z. Naturforsch 13a, 564 (1958), Eine einfach molekularstatische theorie der nematischen kristallinflussign phase, Dispersionswechselwirkung; W. Maier, and A. Saupe, Z. Naturforsch, 14a, 882 (1959), Eine einfach molekularstatische theorie der nematischen kristallinflussign phase. Teil I; W. Maier, and A. Saupe, Z. Naturforsch, 15a, 287 (1960), Eine einfach molekularstatische theorie der nematischen kristallinflussign phase. Teil II; A. Saupe and W. Maier, Z. Naturforsch, 16a, 816 (1961), Methoden zur Bestimmung des Ordnungsgrades nematischer Schichten; W Maier, Angew. Chem. 73, 660 (1961), Struktur und Eigenschaften nematisscher Phasen.

[7] A. L. Tsykalo, Thermophysical Properties of Liquid Crystals, Gordon and Breach Science Publishers, p27 (1991).

[8] K. K. Kobayashi; Phys. Lett. A, 31, 125-126 (1970); On the theory of translational and orientational melting with application to liquid crystals.

[9] W. L. McMillan; Phys. Rev. A 4, 1238-1246 (1971), Simple molecular model for the smectic A phase of liquid crystals.

[10] W. L. McMillan; Phys. Rev.A 6, 936 (1972), X-Ray Scattering from Liquid Crystals. I. Cholesteryl Nonanoate and Myristate.

[11] A. L. Tsykalo, Thermophysical Properties of Liquid Crystals. Gordon and Breach Science Publishers, p 164 (1991).

[12] R. J. Meyer and W. L. McMillan; Phys. Rev. A, 9, 899 (1974), Simple molecular theory of the smectic C, B, and H phases.

[13] S. Chandrashekar; Liquid crystals, Cambridge University Press (1977).

[14] G.Vertogen and W. H. de Jeu; Thermotropic Liquid crystals, Fundamentals. Springer-Verlag, Berlin (1988).

[15] P. J. Collings and Michael Hird; Introduction to Liquid Crystals Chemistry and Physics. Taylot and Francis (1998).

[16] G. R. Luckhurst; Molecular Phhysics of Liquid Crystals, Academic Press (1979).

[17] R. L. Humphries, P. G. James and G. R. Luckhurst; J. Chem. Soc., Faraday Trans. 2, 68, 1031 – 1044 (1972), Molecular field treatment in nematics.

[18] K. K. Kobayashi; J. Phys. Soc. (Japan), 29, 101 (1970), Theory of Translational and Orientational Melting with Application to Liquid Crystals I.

[19] K. K. Kobayashi; Mol. Cryst. Liq. Cryst., 13, 137 (1971), Theory of Translational and Orientational Melting with Application to Liquid Crystals.

[20] B. K. Vainstein; Diffraction of X-rays by Chain Molecules, Elsevier, Amsterdam (1966).

[21] H. Kelkar and R. Hatz; Handbook of Liquid Crystals, Verlag Chemie, Ch. 5 (1980).

[22] P. S. Pershan; Structure of Liquid Crystalline Phases, World Scientific, Singapore (1988).

[23] G. Ungar in Physical properties of liquid crystals, D. A. Dunmur, A. Fukuda and G. R. Luckhurst (Eds.), INSPEC, London, Ch. 4.1 (2001).

[24] G. Vertogen and W. H. de Jeu (Eds.), Thermotropic Liquid Crysatals Fundamentals., Springer-Verlag, p-207 (1988).

[25] G. R. Luckhurst in Liquid Crystals & Plastic Crystals (Eds. G. W. Gray and P. A. Winsor), Ellis Horwood Limited, Vol 2, p-144 (1974).

[26] C. L. Khetrapal and A. C. Kunwar in Advances in Liquid Crystals, Vol. 1-6, Ed. Glenn H. Brown, p-173, AP (1983).

[27] V. D. Neff in Liquid Crystals & Plastic Crystals (Ed. G. W. Gray and P. A. Winsor), Ellis Horwood Limited, Vol 2, p-231 (1974).

[28] S. J. Gupta, R. A. Gharde and A. R. Tripathi; Mol. Cryst. Liq. Cryst., 364, 461- 468 (2001), Phase Transition Temperatures of LCs using Fabry-Perot Etalon.

[29] D. Demus, Textures of liquid crystals, Verlag Chemie Weinheim, New York (1978).

[30] I. Dierking, Textures of liquid crystals WILEY-VCH, GmbH & Co. KGaA p-16 (2003).

[31] A. J. Slaney, K. Takatohi and J. W. Goodby in The Optics of Thermotropic Liquid Crystals, Ed. S. Elston and R. Sambles, Taylor & Francis (1998), Defect textures in liquid crystals.

[32] Y. Bouligand in Handbook of Liquid Crystals. Vol. 1 (Fundamentals), Ed. D. Demus, J. Goodby, G. W. Gray, H.-W. Spiess and V. Vill, WILEY-VCH, Verlag GmbH, Weinheim, FRG (1998), Defects and textures.

[33] B. Jha and R. Paul; Proc. Nucl. Phys. and Solid State Phys. Symp., India . 19C, 491 (1976) A Design for High Temperature X-ray Camera for the Study of Liquid Crystals in a Magnetic Field.

[34] B. Jha, S. Paul, R. Paul and P. Mandal; Phase Transitions, 15, 39-48 (1989), Order parameters of some homologue cybotactic nematics from X-ray diffraction measurements.

[35] S. Diele. P. Brand and H. Sackmann; Mol. Cryst. Liq. Cryst., 16, 105-116 (1972), X-ray Diffraction and Polymorphism of Smectic Liquid Crystals 1. A-, B- and C-modifications.

[36] A. de Vries; Pramana, Suppl. No. 1, 93 (1975), X-Ray Studies of Liquid Crystals: V, Classification of Thermotropic Liquid Crystals and Discussion of Intermolecular Distances.

[37] A. de Vries, A. Ekachi and N. Sielberg; J. de Phys., 40, C3-147 (1979), X-Ray Studies of Liquid Crystals VI. The Structure of the Smectic A, C, Bn and Bt Phases of Trans-1, 4-Cyclohexane-DI-NOctyloxybenzoate.

[38] A. J. Leadbetter, J. Prost, J. P. Gaughan and M. A. Mazid; J. de Phys., 40, C3-185 – C3-193 (1979), The structure of the crystal, SmE and SmB forms of IBPBAC.

[39] A. J. Leadbetter and P. G. Wrighton; J. de Phys., 40, C3-234 – C3-242 (1979), Order parameters in S_A, S_C, and N phases by X-ray diffraction.

[40] V. M. Sethna, A. de Vries and N. Spielberg; Mol. Cryst. Liq. Cryst., 62, 141-153 (1980), X-Ray Studies of Liquid Crystals VIII: A Study of the Temperature Dependence of the Directly Observed Parameters of the Skewed Cybotactic Nematic Phase of Some Bis-(4′-n-Alkoxybenzal) -2-Chloro-1,4-Phenylenediamines.

[41] L.V. Azaroff and C. A. Schuman; Mol. Cryst. Liq. Cryst., 122, 309-319 (1985), X-Ray Diffraction by Cybotactic Nematics.

[42] A. de Vries; Mol. Cryst. Liq. Cryst., 131, 125-145 (1985), The Use of X-Ray Diffraction in the Study of Thermotropic Liquid Crystals with Rod-Like Molecules.

[43] P. Mandal, M. Mitra, S. Paul and R. Paul; Liq. Cryst., 2, 183-193 (1987), X-Ray Diffraction and Optical Studies of an Oriented Schiff's Base Liquid Crystal.

[44] A. de Vries; Mol. Cryst. Liq. Cryst., 10, 219-236 (1970), X-ray photographic studies of liquid crystals I. A cybotactic nematic phase.

[45] A. de Vries; Mol. Cryst. Liq. Cryst., 11, 361-383 (1970), X-Ray Photographic Studies of Liquid Crystals II. Apparent Molecular Length and Thickness in Three Phases of Ethyl-p-Ethoxybenzal-p-Aminobenzoate.

[46] C. Kittle; Intro to Solid State Physics, Wiley Eastern, Chapter 2 (1976).

[47] G. Pelzl in Handbook of Liquid Crystals. Vol. 1 (Fundamentals), Ed. D. Demus, J. Goodby, G. W. Gray, H.-W. Spiess and V. Vill, WILEY-VCH, Verlag GmbH, Weinheim, FRG (1998).

[48] D. A. Dunmur in The Optics of the Thermotropic Liquid Crystals. Ed. S. Elston and R. Sambles, Taylor & Francis (1998).

[49] S. M. Kelly, M. O'Neill; Chapter 1, Liquid Cryatals For Electro-optic Applications.

[50] A. K. Zeminder, S. Paul and R. Paul; Mol. Cryst. Liq. Cryst. 61, 191-206 (1980), Refractive Indices and Orientational Order Parameter of Five Liquid Crystals in Nematic Phase.

[51] M. F. Vuks; Optics and Spectroscopy, 20, 361-368, (1966), Determination of optical anisotropy of aromatic molecules from the double refraction of crystals.

[52] H. E. J. Neugebauer, J. Canad; Phys., 32, 1-8 (1954), Clasius-Mossoti equation for certain types of anisotropic crystals.

[53] S. Chandrasekhar; Liquid Crystals, second edn., Cambridge University Press, Cambridge, p39, (1992).

[54] W. H. de Jeu, Physical Properties of Liquid Crystalline Materials, Ed G. Gray, Gordon and Breach, Vol. 1, p 41 (1980).

[55] P. G. de Gennes; Mol. Cryst. Liq. Cryst. 12, 193-214 (1971), Short Range Order Effects in the Isotropic Phase of Nematics and Cholesterics.

[56] I. Haller, H. A. Huggins, H. R. Lilienthal and T. R. McGuire; J. Phys. Chem., 77, 950 (1973), Order-Related Properties of Some Nematics; I. Haller; Jappl. Phys. Lett., 24, 349 (1974), Alignment and wetting properties of Nematics.

[57] K. Toriyama, K. Suzuki, T. Nakagomi, T. Ishibashi and K. Odawara; J. de Phys, 40, C3-317 (1979), A design of liquid crystal material for multiplexed liquid crystal display.

[58] D. A. Dunmur and W. H. Miller; Mol. Cryst. Liq. Cryst., 60, 281-283 (1980), Dipole-Dipole Correlation in Nematic Liquid Crystals.

[59] R. E. Michel and G. W. Smith; J. Appl. Phys. 45, 3234 (1974), Dependence of birefringence threshold voltage on dielectric anisotropy in a nematic liquid crystals.

[60] C. J. F. Böttcher, Theory of Electric Polarization, 2nd edition, Vol I (1973) and C. J. F. Böttcher and P. Bordewijk, 2nd edition, Elsevier Scientific Publishing Co., Vol II (1978).

[61] W. H. de Jeu and T. W. Lathouwers; Z. Naturforsch 29a, 905 (1974), Dielectric constants and molecular structure of nematics. I. Terminally substituted azobenzene and azoxybenzenes.

[62] W. Maier and G. Meier, Z. Naturforsch; 16a, 262 (1961), Einfache Theorie der dielektrischen Eigenschaften von homogen orientierten nematischen Phasen.

[63] L. Onsager; J. Am. Chem. Soc., 58, 1486-1493 (1936), Electric Moments of Molecules in Liquids.

[64] L. Bata and A. Buka; Mol. Cryst. Liq. Cryst, 63, 307 (1981), Dielecteric Permittivity and Relaxation Phenomena in smectic Phases.

[65] H. Frohlich, Theory of Dielectrics. Clarendon Press, Oxford (1949); H. Frohlich, J. Chem. Phys., 22, 1804 (1954).

[66] P. Bordewijk; Physica, 69, 422-432 (1973), On the derivation of the Kirkwood-Fröhlich equation.

[67] P. Bordewijk; Physica, 75, 146-156 (1974), Extension of the Kirkwood-Fröhlich theory of the static dielectric permittivity to anisotropic liquids.

[68] P. Bordewijk and W. H. de Jeu; J. Chem. Phys. 68 (1), 116 (1978), Calculation of dipole correlation factors in liquid crystals with use of a semiempirical expression for the internal field.

[69] W. H. de Jeu and P. Bordewijk; J. Chem. Phys. 68 (1), 109 (1978), Physiical studies of nematic azoxybenzenes. II. Refractive indices and the internal field.

[70] W. H. de Jeu, T. W. Lathouwers and P. Bordewijk; Phys. Rev. Lett. 32, 40 (1974), Dielectric properties of n and S_A p,p/-di-n-heptylazoxybenzene.

[71] W. H. de Jeu, J. W. A. Goosens and P. Bordewijk; J. Chem. Phys. 61, 1985(1974), Influence of smectic order on the static dielectric permittivity of liquid crystals.

[72] P. Debye, Polar molecules, Dover Pub. Ine., NX (1929).

[73] C. J. F. Böttcher and P. Bordewijk, Ed., Theory of Electric Polarization, Vol II, Dielectric in time-dependent fields, Elsevier, Scientific Publishing Co. (1973).

[74] S. Havriliak and S. Negami; J. Polime, 8, 161-210 (1967), A complex plane representation of dielectric and mechanical relaxation processes in some polymers.

[75] A. Wurflinger; Int. Rev. Phys. Chem., 12, 89 (1993), Dielectric studies under pressure on plastic and liquid crystals.

[76] W. Haase, H. Pranoto, F. J. Bormuth, Ber. Bunsenges. Phys. Chem., 89, 1229-1234 (1985), Dielectric Properties of Some Side Chain Liquid Crystalline Polymers.

[77] F. J. Bormuth, Ph.D. Thesis, Technische Hochschule, Darmstadt (1998).

[78] V. I. Minkin, O. A. Osipov, Y. A. Zhdanov, Dipole Moments in Organic Chemistry, New York- London, (1970).

[79] A. K. Jonscher, Dielectric Relaxation In Solids, Chelsea Dielectric Press, London (1983).

[80] S. Wrobel, B. T. Gowda, W. Haase, J.Chem. Phys., 106 (10), 5904 (1997), Dielectric study of phase transitions in 3-nitro-4-chloro-aniline.

[81] V. K. Agarwal and A. H. Price; Mol. Cryst. Liq. Cryst., 98, 193-200 (1983), Dielectric Relaxation and Order Parameters in Mixtures of 4-cyanobiphenyl and MBBA.

[82] V. V. Daniel, Dielectric Relaxation, Academic Press, London and N.Y. (1967).

[83] K. S. Cole and R. H. Cole; J. Chem. Phys. 9, 341-351 (1941), Dispersion and Absorption in Dielectrics I. Alternating Current Characteristics.

[84] J. Hatano, Y. Hakanai, H. Furue, H. Uehara, S. Saito, and K. Murashiro, Jpn. J. Appl. Phys., 33, 5498-5502 (1994), Phase Sequence in Smectic Liquid Crystals Having Fluorophenyl Group in the Core.

[85] S. Merino, M. R. de la Fuente, Y. Gonzalez, M. A. Perez Jubindo, M. B. Ros, J. A. Puertolas; Phys. Rev., E 54, 5169-5177 (1996), Broadband dielectric measurements on the (R)-1-methylheptyl-6-(4’-decyloxybenzoyloxy)-2-naphthalene carboxylate antiferroelectric liquid crystal.

[86] A. Fafara, B. Gestblom, S. Wrobel, R. Dabrowski, W. Drzewinski, D. Kilian, W. Haase; Ferroelectrics, 212, 79-90 (1998), Dielectric spectroscopy and electrooptic studies of new MHPOBC analogues.

[87] M. Marzec, R. Dabrowski, A. Fafara, W. Haase, S. Hiller and S. Wrobel; Ferroelectrics, 180,127-135(1996), Gold-stone mode and Domain mode relaxation in ferroelectric phases of 4'-[(S.S) - 2,3 - epoxyhexyloxy] Phenyl 4 (Decyloxy) Benzoate (EHPDB).

[88] H. Uehara, Y. Hakanai, J. Hatano, S. Saito and K. Murashiro; Jpn. J. Appl. Phys., 34, 5424-5428 (1995), Dielectric Relaxation Modes in the Phases of Antiferroelectric Liquid Crystals.

[89] M. Buivydas, S. T. Lagerwall, F. Gouda, R. Dubal, A. Takeichi; Ferroelectrics, 212, 55-65 (1998), The dependence of polarization and dielectric biaxiality on the enantiomeric excess in chiral dopant added to a smectic C host mixture.

[90] H. Kresse, H. Schmalfuss, W. Weissflog, C. Tschierske, A. Hauser; Mol. Cryst. Liq. Cryst., 366, 505-517 (2001), Dielectric Characterization of Bn Phases.

[91] W. Kuczynski, Electrooptical studies of relaxation processes in ferroelectric liquid crystals, in: W. Haase, S. Wrobel (Eds), Relaxation phenomena –Springer-Verlag, Berlin-Heidelberg, pp 422-444 (2003), Liquid crystals, magnetic systems, polymers, high-TC superconductors, metallic glasses.

[92] A. M. Biradar, S. Wrobel and W. Haase; Phys. Rev. A, 39 2693-2702 (1989), Dielectric relaxation in the smectic-A* and smectic-C* phases of a ferroelectric liquid crystal.

[93] J. K. Ahuja and K. K. Raina; Jpn. J. Appl. Phys., 39, 4076-4081 (2000), Polarization Switching and Dielectric Relaxations in Ferroelectric Liquid Crystals.

[94] Y. P. Panarin, O. Kalinovskaya, J. K. Vij and J. W. Goodby; Phys. Rev. E, 55, 4345-4353 (1997), Observation and investigation of the ferrielectric subphase with high qT parameter.

[95] I.-S. Baik, S. Y. Jeon, S. H. Lee, K. A. Park, S. H. Jeong, K. H. An, and Y. H. Lee; Appl. Phys. Lett. 87, 263110 (2005), Electrical-field effect on carbon nanotubes in a twisted nematic liquid crystal cell.

[96] F. Haraguchi, K.-I Inoue, N. Toshima, S. Kobayashi, and K. Takatoh; Jpn. J. Appl. Phys. 46, L796 (2007), Reduction of the Threshold Voltages of Nematic Liquid Crystal Electrooptical Devices by Doping Inorganic Nanoparticles.

[97] F. C. Frank; Disc. Faraday Soc., 25, 19-28 (1958), On the theory of liquid crystals.

[98] I. W. Stewart, The Static and Dynamic Continuum Theory of Liquid Crystals, Taylor and Francis, London (2004).

[99] B. Kundu, S. K. Pal, S. Kumar, R. Pratibha, N.V. Madhusudana; Phys. Rev. E: Stat. Nonlinear Soft Matter Phys. 82, 061703 (2010), Splay and bend elastic constants in the nematic phase of some disulfide bridged dimeric compounds.

[100] M. Hird; Liq. Cryst., 38, 1467–1493 (2011), Invited topical review (Ferroelectricity in liquid crystals -materials, properties and applications).

[101] C. B. Sawyer and C. H. Tower; Phys. Rev. 35, 269-273 (1930), Rochelle Salt as a Dielectric.

[102] W. J. Merz; Phy. Rev. 95(3), 690-698 (1954), Domain Formation and Domain Wall Motions in Ferroelectric BaTiO3 Single Crystals; Y. Ouchi, T. Uemura, H. Takezoe and A. Fukuda; Jpn. J. Appl. Phys., 24 (4), L235- L238 (1985), Correspondence between Stroboscopic Micrographs and Spontaneous Polarization Measurements in Surface Stabilized Ferroelectric Liquid Crystal Cells.

[103] W. J. Merz; J. Appl. Phys. 27(8), 938-943 (1956), Switching Time in Ferroelectric BaTi03 and Its Dependence on Crystal Thickness.

[104] H. D. Megaw; Acta Cryst., 7,187-194 (1954), Ferroelectricity and crystal structure II.

[105] M. E. Lines and A. M. Glan; Oxford, Clarendon 128 (1977), Principles and Applications of Ferroelectric and Related Materials.

[106] K. Miyasato, S. Abe, H. Takezoe, A. Fukuda and E. Kuze; Jpn. J. Appl. Phys. 22 (10), L661-L663 (1983), Direct Method with Triangular Waves for Measuring Spontaneous Polarization in Ferroelectric Liquid Crystals.

[107] S. Kaur, A. K. Thakur, R. Chauhan, S. S. Bawa and A. M. Biradar; Physica B, 352, 337-341 (2004), The effect of rotational viscosity on the memory effect in ferroelectric liquid crystal.

[108] S. S. Bawa, A. M. Biradar and S. Chandra; Jpn. J. Appl. Phys. 25(6), L446 (1986), Frequency Dependent Polarization Reversal and the Response Time of Ferroelectric Liquid Crystal by Triangular Wave Method.

[109] J-Z. Zue, M. A. Handschy and N. A. Clark; Ferroelectrics, 73, 305-314 (1987), Electrooptic response during switching of a ferroelectric liquid crystal cell with uniform director orientation.

[110] K. Skarp, I. Dahl, S. T. Lagerwall and B. Stebler; Mol. Cryst. Liq. Cryst., 114, 283-297 (1984), Polarization and Viscosity Measurements in a Ferroelectric Liquid Crystal by the Field Reversal Method.

[111] T. Carlsson, B. Zeks, C. Filipic, A. Levstik; Physical Review A, 42, 877–889 (1990), Theoretical model of the frequency and temperature dependence of the complex dielectric constant of ferroelectric liquid crystals near the smectic C^* - smectic A phase transition.

[112] J. D. Bernal and D. Crowfoot; Trans. Farad. Soc., 29, 1032-1049 (1933), Crystalline phases of some substances studied as liquid crystals.

[113] P. Mandal and S. Paul; Mol. Cryst. Liq. Cryst., 131, 223-235 (1985), X-Ray Studies on the Mesogen $4^{/}$-n-Pentyloxy-4-Biphenylcarbonitrile (5OCB) in the Solid Crystalline State.

[114] P. Mandal, S. Paul, H. Schenk and K. Goubitz; Mol. Cryst. Liq. Cryst., 135, 35-48 (1986), Crystal and Molecular Structure of the Nematogenic Compound 4-Cyanophenyl-4'-n-Heptylbenzoate (CPHB).

[115] P. Mandal, B. Majumdar, S. Paul, H. Schenk and K. Goubitz; Mol. Cryst. Liq. Cryst., 168, 135-146 (1989), An X-ray Study of Cyanophenyl Pyrimidines, Part I - Crystal Structure of PCCPP.

[116] P. Mandal, S. Paul, C. H. Stam and H. Schenk; Mol. Cryst. Liq. Cryst., 180, 369-378 (1990), X-Ray Studies of Cyanophenyl Pyrimidines Part II The Crystal and Molecular Structure of 5-(4-Ethylcyclohexyl)-2-(4-Cyanophenyl) Pyrimidine.

[117] S. Gupta, P. Mandal, S. Paul, M. de Wit, K. Goubitz and H. Schenk; Mol. Cryst. Liq. Cryst., 195, 149-159 (1991), An X-Ray Study of Cyanophenylpyrimidines Part III. Crystal Structure of 5-(trans-4-Heptylcyclohexyl)-2-(4-Cyanophenyl) Pyrimidine.

[118] P. Mandal, S. Paul, H. Schenk and K. Goubitz; Mol. Cryst. Liq. Cryst., 210, 21-30 (1992), Crystal and Molecular Structure of a Cybotactic Nematic Compound bis-(4’-n-Butoxybenzal)-2-Chloro-l,4-Phenylinediamine.

[119] P. Mandal, S. Paul, K. Goubitz and H. Schenk; Mol. Cryst. Liq. Cryst., 258, 209-216 (1995), X-ray Structural Analysis of a Mesogenic Compound N,N'-Bis-(p Butoxybenzy1idene)-α, α'- bi - p-To1uidine.

[120] A. Nath, S. Gupta, P. Mandal, S. Paul and H. Schenk; Liq. Cryst., 20, 765-770 (1996), Structural analysis by X-ray diffraction of a non-polar alkenyl liquid crystalline compound.

[121] B. R. Jaishi, P. K. Mandal, K. Goubitz, H. Schenk, R. Dabrowski and K. Czuprynski; Liq. Cryst., 30, 1327-1333 (2003), The molecular and crystal structure of a polar mesogen 4-cyanobiphenyl-4'-hexylbiphenyl carboxylate.

[122] P. A. C. Gane and A. J. Leadbetter; Mol. Cryst. Liq. Cryst., 78, 183-200 (1981), The Crystal and Molecular Structure of N- (4- n octyloxy benzylidene) -4'-butylaniline (80.4) and the Crystal-Smectic G Transition.

[123] L. Malpezzi, S. Bruckner, D. R. Ferro and G. R. Luckhurst; Liq. Cryst., 28, 357-363 (2001), Crystal structure and packing analysis of the liquid crystal dimer α,ω-bis(4-cyanobiphenyl-4'-yloxy)octane.

[124] M. A. Sridhar, N. K. Lokanath, J. Shashidhara Prasad, C. V. Yelammagad and Varshney, Liq. Cryst., 28, 45-49 (2001), Crystal structure of a cholesterol-based dimesogen.

[125] V. K. Gupta, P. Bhandhoria, M. Kalyan, M. Mathews and C. V. Yelamaggad; Liq. Cryst., 32, 741-747 (2005), Crystal structure of a liquid crystal non‐symmetric dimer: cholesteryl 4‐[4‐(4‐n‐butylphenylethynyl) phenoxy]butanoate.

[126] L. Walz, F. Nepveu and W. Haase; Mol. Cryst. Liq. Cryst., 148, 111-121 (1987), Structural Arrangements of the Mesogenic Compounds 4-Ethyl-4'-(4"-pentylcyclohexyl) biphenyl and 4-Ethyl-2'-fluoro-4'-(4"-pentylcyclohexy1) biphenyl (BCH's) in the Crystalline State.

[127] P. S. Patil, V. Shettigar, S. M. Dharmaprakash, S. Naveen, M. A. Sridhar and J. Shashidhara Prasad, Mol. Cryst. Liq. Cryst., 461, 123-130 (2007), Synthesis and Crystal Structure of 1-(4-fluorophenyl)-3-(3,4,5-trimethoxyphenyl)-2-propen-1-one.

[128] R. F. Bryan, Proceedings of the Pre-Congress Symposium on Organic Crystal Chemistry, Poznan, Poland, 105 (1979); J. Structural Chem., 23, 128 (1982).

[129] W. Haase and M. A. Athanassopoulou; Liquid Crystals, D.M.P. Mingos (Ed.), Springer-Verlag, Vol. I, pp. 139-197 (1999).

[130] S. Biswas, S. Haldar, P. K. Mandal, K. Goubitz, H. Schenk, and R. Dabrowski; Cryst. Res. Technol. 42, 10, 1029-1035 (2007), Crystal structure of a polar nematogen 4-(trans-4-undecylcyclohexyl) isothiocyanatobenzene.

[131] S. Haldar, S. Biswas, P. K. Mandal, K. Goubitz, H. Schenk and W. Haase; Mol. Cryst. Liq. Cryst., 490, 80–87 (2008), X-Ray Structural Analysis in the Crystalline Phase of a Nematogenic Fluoro-Phenyl Compound.

[132] S. Haldar, P. K. Mandal, S. J. Prathap, T. N. Guru Row and W. Haase; Liq. Crys., 35, 11, 1307–1312 (2008), X-ray studies of the crystalline and nematic phases of 49-(3,4,5-trifluorophenyl)-4-propylbicyclohexyl.

[133] P. Das, A. N. Biswas, S. Acharya, A. Choudhury, P. Bandyopadhyay, P. K. Mandal and S. Upreti; Mol. Cryst. Liq. Cryst., 501, 53–61 (2009), Structure of Liquid Crystalline 1-Phenyl-3-{4-[4-(4-octyloxybenzoyloxy)phenyloxycarbonyl]phenyl}triazene-1-oxide at Low Temperature.

[134] B. K. Vainshtein, Diffraction of X-rays by Chain Molecules, Elsevier, Amsterdam, p12 (1966).

[135] M. F. C. Ladd and R. A. Palmer, Theory and practice of Direct methods in Crystallography, Plenum Pub. Co., N. Y., (1980).

[136] G. Germain, P. Main and M. M. Woolfson; Acta Cryst., B26, 274-285 (1970), On the application of phase relationships to complex structures.

[137] H. Schenk and C. T. Kiers, Simpel 83, an automatic direct method program package, University of Amsterdam (1983); H. Schenk; Recl. Trav. Chim. Pays-bas, 102, 1(1983).

[138] G. M. Sheldrick, Direct method package program, University of Gottingen, Germany (1993).

[139] S. R. Hall and J. M. Stewart, XTAL, University of Western Australia and Maryland (1989).

[140] A. Altomere, G. Cascarano, C. Giacovazzo, A. Guagliardi, M. C. Burla, G. Polidori and M. Camalli, The SIR 92 Programme (1992).

[141] P. S. White, PC Version of NRCVAX (88), University of New Brunswick, Canada (1988).

[142] Yao Jia-Xing, Zheng Chao-de, Quian Jin-Zi, Han Fu-Son, Gu Yuan-Zin and Fan Hai-Fu, SAPI: A Computer Program for Automatic Solution of Crystal Structures from X-ray Data, Institute of Physics, Academia Sinica, Beijing (1985).

[143] C. J. Gilmore, J. App. Cryst., 17, 42-46 (1984), MITHRIL-an integrated direct-methods computer program.

[144] H. Hauptman and J. Karle, Acta Cryst., 9, 45-55 (1956), Structure invariants and seminvariants for noncentrosymmetric space groups; ibid., 12, 93-97 (1959); Seminvariants for centrosymmetric space group with conventional centered cells.

[145] J. Karle and H. Hauptman, Acta Cryst., 14, 217-223 (1961), Seminvariants for non-centrosymmetric space groups with conventional centered cells.

[146] J. Karle and I. L. Karle, Acta Cryst., 21, 849-859 (1966), The symbolic addition procedure for phase determination for centrosymmetric and non-centrosymmetric crystals.

[147] H. Schenk (Ed), Direct Methods in Solving Crystal Structures, NATO ASI Series, Plenum Press, New York (1991).

[148] G. H. Stout and L. H. Jensen, X-ray Structure Determination, Macmillan, New York p195 (1968).

[149] A. J. C. Wilson, Nature, 150, 152 (1942), Determination of Absolute from Relative X-Ray Intensity Data.

[150] W. Cochran and M. M. Woolfson, Acta Cryst., 8, 1-12 (1955), “The theory of sign relations between structure factors”.

[151] W. Cochran, Acta Cryst., 8, 473-478 (1955), Relations between the phases of structure factors.

[152] J. Karle and H. Hauptman, Acta Cryst., 9, 635-651 (1956), A theory of phase determination for the four types of non-centrosymmetric space groups.

[153] M. J. Buerger, Crystal Structure Analysis, Wiley, New York (1960).

[154] G. H. Stout and L. H. Jensen, X-ray Structure Determination, Macmillan, New York, p353 (1968).